The Peptide Dynamics Project

A scientific research endeavor to study the dielectric spectra of peptides and proteins.

Infinite Quanta, Inc.

A Non-Profit (IRC 501(c)(3)) Scientific Research Organization

Stephen J. Lukacs Jr., Ph.D., President, and Principle Investigator

The Cathedral

Overall Purpose & General Approach

Imagine a medical instrument similar in scale and function to a Magnetic Resonance Imager (MRI). The instrument would be able to observe disease within the body, and then, additionally direct the healing process without drugs or surgical intervention. A medical instrument conforming to this vision would employ a field capable of penetrating the spatial depths and organs of the body. It would also have the capability for manipulating and directing the molecular engines and mechanisms, i.e., proteins and enzymes, of the organism. There are only a few energy fields available to science. The electric field appears to offer the best means for achieving the proposed instrument.

Electrical energy is the most important physical energy in our daily lives. It powers our homes and is responsible for carrying information on our telephones and the internet. What if electrical energy can be used to derive a greater understanding of our bodies and health? What if the electric field is the key to understanding the deeper aspects of life within the disciplines of biophysics, biochemistry, molecular biology, microbiology, proteomics, genetics, medicine and life, itself?

The interaction of electric fields with molecules is known as dielectrics. Dielectric materials have been studied since the mid 1800's. This discipline should be applicable to the modern understanding of proteins using modern electronic and computational techniques. An electric field appears to offer the greatest opportunity for directly observing and categorizing larger scale sub-domains, called structural motifs, within a protein. Such instrumentation would be comparable to "current arts" in biochemistry, i.e., Nuclear Magnetic Resonance (NMR) and Infra-Red (IR) Spectroscopy. The dielectric responses from proteins will lead to relaxation and resonance signatures. Such signatures could direct an electric waveform to manipulate protein function and catalysis, thereby stimulating the body to heal.

Spectroscopy allows observation of the frequency response of an electric field with matter. For example, infra-red (IR) spectroscopy uses the response of molecular vibrations of bonded atoms to an applied electric field. Essentially, the bonded atoms absorb energy from the applied electric field. IR spectroscopy allows for the observation of the absorbed energy. Early developers of IR spectroscopy attributed each distinct frequency response to various bond stretches, bends, and rotations to create a reproducible catalog of atomic responses within the molecule. The IR table of responses is well-known to any second-year chemistry student and synthetic research chemist. For, when a peak is observed, we can attribute that response to a certain atomic motion, or organic functional group, within the molecule. Two examples are the carbon-hydrogen stretch in methane and the amide bond in peptides. Therefore, IR Spectroscopy has provided modern scientists with a standard, reliable, and routine technique for studying molecular structures and mechanisms.

Dielectric spectroscopy encompasses much lower frequencies, microwave and lower, than IR spectroscopy. It offers the potential for observing larger structural domains within molecules, or whole molecular responses and processes. Dielectric spectroscopy is based on charge differentials, or dipoles, interacting with the applied electric field. Dipoles can have a very local field-of-view, focusing on single atoms, larger sub-domains within molecules, or whole molecular responses. Each dimension will respond differently to the applied electric field leading to a categorization of molecular dipolar

responses. The proposed dielectric instrumentation development is similar to early IR spectroscopic development.

Proteins are large molecules, composed of thousands of atoms, which possess large sub-domains called structural motifs. These prevalent motifs, such as α-helices and β-sheets, have been studied for decades. They possess very definite dipolar characteristics. For instance, a particular protein is composed of eight α-helical regions, but another protein has three α-helical and four β-sheet regions. Each region has different dipolar characteristics which should be directly observable with dielectric spectroscopy.

It is the objective of this project to build dielectric spectrometers and develop the techniques for studying the intramolecular dipolar responses of structural motifs within peptides and proteins. Such studies are analogous to using an electrical surgical knife to probe the internal molecular structure, or "organs", of peptides and proteins. Each motif should resonate at a particular frequency complying with that of the applied electric field. This will provide a unique "fingerprint" for the relaxation or resonance signature. The categorized signatures will allow researchers to introduce complex electric field waveforms, pulses, and wave packets to influence and manipulate the motifs of the protein. This will control the structural and catalytic nature of the protein without invasive methods, such as drug or surgical interventions.

Practical Applications

In the same way IR Spectroscopy is a pervasive and routine laboratory technique, we envision the PDP as developing the instrumentation and techniques to create a catalog of dielectric responses for characterizing the secondary structure and intramolecular structural motifs of proteins. The characterization of such secondary structure will include intrinsic structural and intra- and interchain dynamics of proteins. Therefore, this endeavor would provide such instrumentation to the college student or research scientist for studying proteins as routinely as studying alkanes with IR Spectroscopy.

For example, a scientist would be able to see the transitions of an α-helical peptide to a random coil by changing the temperature, pH, or salinity of the solution as denaturation occurs. These initial studies would extend to observing the hydration layers in and around a large complex protein. Then, allowing the scientist to see the individual structural motifs and their interchain interactions under varying environmental conditions. This basic understanding would advance the fields of biophysics and biochemistry.

These studies would form a basis for frequency-dependent markers of the intrinsic intramolecular dielectric response of peptides and proteins. A catalog of markers would allow for the qualitative and quantitative observation of markers, and the transitions from one marker to the next. This potential avenue for dielectric instrumentation would advance the science of proteomics; or, the identification, assembly, and static and dynamic characterization of all proteins involved in a particular anabolic or catabolic pathway.

The dielectric markers and proteomic instrumentation would allow, for example, a scientist to study the post-translational modification leading to the completely assembled and functional protein or enzyme, or the conformational changes of an enzyme during a reaction, a membrane bound passive ion channel, or

an active protein pump. The scientist will have the tools to study the intramolecular structural transitions of the protein as its carrier passes through the channel.

Huge macromolecules, such as immunoglobins, can be structurally, dynamically, or conformationally studied with such a dielectric proteomic instrument. Such macromolecular studies would allow for organelle or cellular studies. The instrumentation and studies can, for example, contribute to sickle cell versus non-sickle cell diagnosis and drug treatment. The lipoprotein precursors of cardiovascular condition and treatment can be traced through the dielectric proteomic instrumentation.

A scientist would be able to see how a drug affects the conformational and transitional states of a protein in its natural aqueous environment. The low-energy non-evasive, and eventually *in vivo*, technique will dramatically affect medicine and pharmaceuticals. Perhaps, the technique will lead to directly manipulating single proteins, or sets of proteins, within the body to perform cellular repair, thus inducing the healing process.

Or, once the dynamical processes of protein structure is better understood, then bio- and nanoengineers can synthesize proteins, such as synthetic blood, and molecular machines that are ten million times smaller than your finger nail, but designed and built to perform a specific task.

Since the pure research endeavor of the PDP is so profound, the practical applications are far reaching. The primary focus of the PDP at this point, is to successfully develop the instrumentation for the proper and reproducible categorizing of the secondary structure and intramolecular structural motifs of peptides and proteins. Such an instrument would profoundly affect our biophysical, biochemical, and proteomic understanding of living systems, and consequently affect, micro- and molecular cell biology, immunology, endocrinology, pharmacology, bioengineering, and nanotechnology.

Current Project Status

The first generation Phase I Dielectric Spectrometer (P1DS) with a frequency range of 1 mHz to 250 kHz, has been built and tested in my personal laboratory. It has generated uncompromising results for gelatin, myoglobin, and hemoglobin. However, the electronics, sample holders, experimental controls, computer hardware and software must be upgraded to see deeper into the proteins. Phase II through IV Dielectric Spectrometers are currently being developed to encompass a frequency range of 1 μHz to 15 GHz. These three dielectric spectrometers will provide greater stability, sensitivity, frequency range, and reproducibility then has ever been achieved so far.

Abstract

Protein energetics have been classically studied by the excitation of a chromophore bound to the protein. The inherent chromophores include UV-active amino acids embedded within the primary structure of the peptide or chemically-bonded optically-active metal or organic prosthetic groups. These techniques have been used to successfully study regions of a protein and the respective quenching mechanisms of the excited inherent chromophores.

Impedance or dielectric spectroscopy is an ultra-low energy technique based on the capacitive response of a sample. A real capacitor exhibits both the capability to effectively store charge (dispersive) and dissipate energy (absorptive) from an external time-varying electric field. A well designed dielectric spectrometer will simultaneously measure both the dispersive and absorption responses of the sample versus incident frequency. Dielectric spectroscopy has been used in the last decade to study organic solvents, solid-state materials and devices, corrosion, thin-films, and coatings.

The primary structure of all peptide chains exhibit a permanent dipole moment based on the positive charge of the amine group and the negative charge of the carboxylic group of every amino acid in the chain and those electric dipoles based on the polar R groups laterally from the primary chain. The secondary and tertiary folding will further enhance or diminish the local dipoles into a net permanent dipole moment, or a series of local permanent dipole moments. Every protein possesses a permanent dipole moment which could in principle be directly studied by dielectric spectroscopy.

It is our proposal to build a custom dielectric spectrometers with enough sensitivity, down to 2 fA, or better, and a spectral range, 1 μHz to 15 GHz, to directly observe and characterize the intramolecular dipole moments of peptides and proteins. This technique will study the protein itself, and not only be limited to only the UV- or optically-active chromophores. The characterization of such dipole moments will allow for the empirical deduction of the hydrophobic and hydrophilic interactions and local internal environments of the proteins' secondary and tertiary structures. The empirical data gathered from these interactions and environments will allow for further qualitative and quantitative characterization of structural motifs such as α-helices, β-sheets, and hairpin bends, as well as, enzymatic, antibiotic, and hormonal active sites.

The beforementioned empirical data will eventually lead to permanent molar polarization and structural motif catalogs of spectral responses that will be invaluable in biophysics, biochemistry, proteomics, micro- and molecular cell biology, immunology, endocrinology, pharmacology, bioengineering, and nanotechnology.

Introduction

Life, in its entirety, is based on some fairly simple classes of chemical compounds: water, salts and some metals, lipids, amino and nucleic acids. For example, the most simple speck of life is a virus. Generally, viruses are composed of an outer protein coat surrounding an inner DNA or RNA strand. Proteins and DNA are the biological analogs of polymers. The basic subunits of proteins are amino acids and those of DNA or RNA are nucleic acids. There are twenty amino acids and five nucleic acids. These subunits can bond to form biopolymeric chains numbering in the millions. Although DNA or RNA are necessary for cellular replication and the propagation of a species genome and phenotypic characteristics, these comprise less than one percent of an entire organism. Proteins, however, comprise the structural, protective, catalytic, and metabolic core of an organism. It is proteins, and their diverse and complex role in life, that inspires the Peptide Dynamics Project, herein known as the PDP.

Any motion of an object with mass within a potential exhibits energy. Energy is the most fundamental observable property of the universe. Energy can do work, produce a force, and change the state of matter. For example, the frictional force of walking will create a small amount of heat in the foot print and the bottom of the shoe, which can be measured with a sensitive thermometer, thermocouple, or infrared detector.

A system will react when different forms or levels of energy are imposed upon it. The observation and measurement of the system's response to the imposed energy will reveal new quantum mechanical properties and chemical characteristics of the system. Additionally, the flow of the imposed energy will reveal how the excess energy moves through the system, for the system will naturally dissipate the energy to return to its most relaxed state. An example of this is when light hits the chlorophyll pigment of a leaf. The absorbed energy is immediately captured and converted into chemical (ATP) energy, which is directly usable by the cell of the plant.

All normal matter is a vast empty black space, a void, with positive nuclei more than a thousand times smaller than the atom itself, and the negative electron orbitals creating the outer envelope of the atom. Matter is nothing more than a sea of moving invisible charge and all stuff, all stuff, is made of matter. Positive nuclei are swimming in a quantized sea of negative electron orbitals. Therefore, it is natural to study this sea of charge potential with an electric field, the most simple probe for studying charge known to science. Impedance or dielectric spectroscopy is the technique of imposing an electric field and studying its effect on a sample or material.

Classical spectroscopic techniques have imposed high energy levels on peptides and proteins in the infrared, visible, and ultra-violet electromagnetic regions to locally excite specifically bound chromophores, i.e. IR, UV-Vis, and laser spectroscopies. It is the intention of the PDP to impose ultra-low, sub-radio, electromagnetic energy to peptide segments and entire proteins and observe the dissipation of the absorbed energy throughout the system. This sub-radio technique is known as impedance or dielectric spectroscopy. Dielectric spectroscopy is an advancement in measuring the complex capacitance of a sample.

The development of infrared spectroscopy included a period of experimentation to empirically categorize specific energy signatures with organic functional groups and interactions, such as the

presence of a methyl group or the steric hindrance of neighboring freely rotating methyl groups. Ultimately, the hope of the PDP is to perform a similar cataloging of peptide groups and protein structural motifs to specific energy signatures using impedance spectroscopy. The PDP Catalog will then be used to study unknown responses in unknown proteins or other biomolecules, or to further study enzymatic, receptor, or binding-site interactions.

The PDP website and proposal are written for a broad audience. The sections are divided to meet the needs of various interests and levels of scientific expertise. Each section is designed to provide an in-depth analysis of impedance spectroscopy, proteins, and the expected response from these systems of study and this instrumental technique.

Theoretical

Theoretical models develop over time. The early versions of the model lay the foundation and the broad strokes on the canvas. As the understanding deepens, the models will converge with empirical results leading to finer and finer strokes, revealing a complete work.

This is the case with electric polarization on dielectrics, beginning with Maxwell and Mossotti in the 1850's, to Debye's 1929 ground breaking work on polar molecules, and finally, to Onsager and Kirkwood on polar liquids. Drude, Debye, and Cole's work on anomalous dispersion and dielectric loss continued the model for dielectrics in a frequency-dependent alternating electric field. Each contribution advances our microscopic understanding of an electric field with polar molecules, and their local solvent environments.

Induced and Orientational Dipoles

Clausius-Mossotti

An external electric field applied to a nonconductive dielectric solid, liquid, solution, or gas will invoke a complex impedance or capacitance. The capacitance of a material is its ability to store charge as imposed by the applied electric field. The bulk material will respond with a polarization given by Maxwell's equation

$$\vec{D} = \varepsilon\vec{E} = \varepsilon_0\vec{E} + \vec{P}$$

(eq. T01)

where D is the electric displacement field, ε is the relative permittivity of the bulk material, ε_0 is the permittivity of free space, E is the applied electric field, and P is the bulk polarization. The bulk polarization is further characterized by

$$\vec{P} = \frac{1}{\Delta V}\sum_i \vec{p}_i$$

(eq. T02)

or, the bulk polarization, P, is the average of all dipole moments, p_i, within a unit volume, V.

The latter equations clarify that the macroscopic electrical measurement, through D, of the bulk sample is directly related to the microscopic, and later proved molecular, response of either induced or permanent electric dipoles, p_i. This treatment will therefore, attempt to bridge the gap between the directly-observed macroscopic response with a microscopic molecular characteristic and physical understanding.

Additionally, this study will focus on peptides and proteins in solution, therefore the following treatment assumes the sample to be linear, isotropic, and homogeneous in response to the applied electric field. An aqueous solution or liquid sample would inherently posses an isotropic and homogenous response. A linear response for such samples would additionally require that the applied electric field, E, be sufficiently small so as to not induce further perturbations, and thus nonlinear terms, into the polarization.

Barger's [Barger, 1987 #107] and Feynman's [Feynman, 1989 #106] approach of quantifying the polarization was to generalize the fields imposed on single molecules with spherical volumes within the dielectric material. The total electric field within the spherical volume would be a culmination of the macroscopically applied electric field and the electric fields of the surrounding volume by the bulk material. The latter electric fields would be those contributions by surrounding dipoles, and since these dipoles would also be aligned by the applied electric field, their contribution to the spherical volume would not be zero. Therefore, the electric field within the spherical volume is the additive effect of both the applied electric field and that of the surrounding dipole moments.

Jackson [Jackson, 1998 #108] specifically imposes the spherical volumes into molecules, in which the small spherical volume is a single molecule. The electric field imposed on the single molecule, E_m, within its spherical volume, is composed of the applied electric field, E, and those molecular dipoles, E_p, surrounding the single molecule, or

$$\vec{E}_m = \vec{E} + \vec{E}_p$$

(eq. T03)

Since E is simply the applied electric field, which is time-varying or sinusoidal, the understanding of the of the electric field on the molecule, E_m, begins with an in depth understanding of the additional electric field by the surrounding dipole, E_p. This begins with the polarization surface charge density

$$\sigma_p = \vec{P} \cdot \hat{n} = P \cos\theta$$

(eq. T04)

and the electric field at the center of the single molecule, or

$$E_p = -\frac{1}{4\pi\varepsilon_0} \int \frac{\sigma(\vec{r}')\hat{n} dS}{R^2}$$

(eq. T05)

If $\hat{n} \cdot \hat{z} = \cos\theta$ and $dS = R^2 \sin\theta d\theta d\phi = -R^2 d(\cos\theta) d\phi$ then

$$E_p = -\frac{1}{4\pi\varepsilon_0}\int\frac{[P\cos\theta][\cos\theta][-R^2 d(\cos\theta)d\phi]}{R^2}$$

$$E_p = +\frac{P}{4\pi\varepsilon_0}\int_0^{2\pi} d\phi \int_{-1}^{+1}\cos^2\theta\, d(\cos\theta)$$

(eq. T06)

which simplifies to

$$\vec{E}_p = \frac{\vec{P}}{3\varepsilon_0}$$

(eq. T07)

To further the treatment, it is customary [Barger, 1987 #107] to parameterize the induced dipole moment, or the dipole moment induced by the applied electric field, as

$$\vec{p} = \alpha\vec{E}_m$$

(eq. T08)

on the molecular scale, α is known as the total polarizability and is an empirical parameter or proportionality constant. The bulk material scale, the average dipole moment per unit volume would follow as

$$\vec{P} = n_v\alpha\vec{E}_m$$

(eq. T09)

where n_v is the number of molecules per unit volume. Substituting the latter with Eq. T07 into Eq. T03 gives

$$\vec{P} = \left(\frac{3n_v\alpha\varepsilon_0}{3\varepsilon_0 - n_v\alpha}\right)\vec{E}$$

(eq. T10)

Macroscopic dielectric materials exhibit the observable parameters: the dielectric constant, the relative permittivity, and the electric susceptibility. These are related to the bulk polarization and the applied electric field as follows

$$\vec{P} = \varepsilon_0(\kappa - 1)\vec{E} = \chi\vec{E}$$

(eq. T11)

where the dielectric constant, $\kappa = \varepsilon/\varepsilon_0 = C/C_0 = \varepsilon_r$, also known as the relative permittivity, and χ is the electric susceptibility. Equating Eq. T10 with Eq. T11 and simplifying gives

$$\kappa = \frac{1 + 2n_v\alpha/(3\varepsilon_0)}{1 - n_v\alpha/(3\varepsilon_0)}$$

(eq. T12)

which is first developed by Mossotti [Mossotti, 1850 #177] in 1850 and independently by Clausius [Clausius, 1879 #178] in 1879 and is called the Clausius-Mossotti equation. This equation reveals the macroscopic dielectric constant, κ, in terms of the microscopic parameter and molecular polarizability, α. Its more traditional form is [Shoemaker, 1989 #101]

$$\left(\frac{\kappa - 1}{\kappa + 2}\right)\frac{M}{\rho} = \frac{N_A}{3\varepsilon_0}\alpha$$

(eq. T13)

where M and ρ is the molecular weight and density of the pure sample, respectively, and N_A is Avagadro's number. The latter is the simple substitution of $n_v = N_A\rho/M$ into Eq. T12.

Debye-Langevin

The total polarizability, α, is not quite as detailed a molecular property as required. The deeper understanding requires to delve into the physical mechanisms and molecular characteristics that comprise the total polarizability.

The molecular model of matter is crucial to understanding the total polarizability. Molecules are composed of at least two electrical components. The atomic nonbonding shells and nonpolar molecular bonds may electrically polarize induced by the applied electric field. Polar molecules will additionally exhibit a permanent dipole moment. Water is a classic example of a polar molecules and most polar molecules are water soluble. Therefore, the total polarizability would be given by

$$\alpha = \alpha_d + \alpha_\mu$$

(eq. T14)

where α_d is the induced polarization of nonpolar and polar submolecular entities alike, and α_m is the orientational or rotational polarization based on the permanent dipole moment of polar molecules. The latter will, of course, be zero for nonpolar molecules. In like manner, the macroscopic response would follow from the bulk polarization, or

$$P_m = P_d + P_\mu$$

(eq. T15)

where P_m is the total or molar polarization, P_d is the induced molar polarization of the electric and atomic polarizability, α_d, and P_μ is the permanent molar polarization of the orientational polarizability leading to the permanent dipole moment, μ.

The treatment of P_d and α_d is inherent to the derivation of the Clausius-Mossotti equation. However, to quantify the orientational polarizability, α_μ, and thus follows P_μ, begins with the potential energy, U_μ, of the permanent dipole moment, μ, in the applied electric field, E, or

$$U_\mu = -\vec{\mu} \cdot \vec{E} = -\mu E \cos\theta$$

(eq. T16)

for a single dipole moment.

Coherence is the state of alignment of the permanent dipole moment with the applied electric field. This is expressed in the latter equation, Eq. T16. A perfectly coherent dipole will possess the greatest coupling to the applied field and exhibit the greatest polarization. Clearly the average bulk polarization is temperature dependent because collisions or vibrations of neighboring molecules will tend to disrupt a coherent dipole. [Schwartz, 1972 #109] Therefore, the additional treatment of the permanent dipole moment into the Clausius-Mossotti equation must allow for the inclusion of statistical mechanics.

The average dipole moments throughout the bulk liquid or solution is applied to the Boltzmann distribution via [Atkins, 1978 #110]

$$\mu_{average} = \mu L(x)$$

(eq. T17)

where L(x) is the Langevin function given by

$$L(x) = \frac{e^x + e^{-x}}{e^x - e^{-x}} - \frac{1}{x} = \coth(x) - \frac{1}{x}$$

(eq. T18)

where $x = \mu E/kT$, k is the Boltzmann constant, and T is the temperature. The Langevin function expands in a taylor series as

$$L(x) = \frac{1}{3}x - \frac{1}{45}x^3 + \frac{2}{945}x^5 - \frac{1}{4725}x^7 + \cdots$$

(eq. T19)

in which it can be seen that the first term is the only major contributing term and thus the average molecular dipole moment, from Eq. T17, is then

$$\mu_{average} \cong \frac{\mu^2 E}{3kT}$$

(eq. T20)

which follows the polarization as

$$\vec{P} = \frac{N_A \mu^2 \vec{E}}{3kT}$$

(eq. T21)

Substituting the latter equation and Eq. T14 into the Clausius-Mossotti equation, Eq. T13, gives the Debye-Langevin equation

$$P_m \equiv \left(\frac{\kappa - 1}{\kappa + 2}\right)\frac{M}{\rho} = \frac{N_A}{3\varepsilon_0}\left(\alpha_d + \frac{\mu^2}{3kT}\right) = P_d + P_\mu$$

(eq. T22)

Direct application of the latter equation yields direct measurement of P_m, via κ, M, and ρ, plotted against 1/T has the form of a straight line. The y-intercept of the line leads to the induced polarization, α_d, and the slope to the permanent dipole moment, μ.

Lorentz-Lorenz

The latter direct application works excellent for gases, however, the temperature range of liquids and solutions will not be as great, therefore, a second method exists to subtract the induced polarizability, α_d, from the total polarizability via the refractive index, n, where

$$\kappa = n^2$$

(eq. T23)

and therefore, at IR or visible electromagnetic frequencies greater than the permanent molar polarization, P_μ, goes to zero and the induced molar polarization, P_d, remains, thus

$$R_m \equiv \left(\frac{n^2 - 1}{n^2 + 2}\right)\frac{M}{\rho} = \frac{N_0}{3\varepsilon_0}\alpha_d = P_d$$

(eq. T24)

known as the Lorentz-Lorenz equation and R_m is the molar refraction. Determination of P_d, at high visible frequencies, can be performed with a Abbe's Refractometer. P_m is then determined for low

frequencies which includes P_μ, in which P_μ is then found by $P_m - P_d$. The permanent dipole moment, μ, then follows from P_μ.

In summary, the macroscopic dielectric response to an applied electric field is based on the microscopic induced polarizable atoms and the permanent dipole moments of molecules. The induced responses represent atomic and nonpolar molecular polarizability and occurs at low and high frequencies of the applied field. The permanent dipole responses represent only polar molecules in which the molecules become rotationally oriented with low frequency electric fields.

Onsager

Kirkwood

Anomalous Dispersion and Absorption

The above treatment provides a basis in which the observed bulk response to an applied electric field relates to its underlying molecular polarizabilities and permanent dipole moments. The above treatment assumes that the applied electric field is static or at extremely low frequencies, thus negating any temporal mechanisms. This section will provide the basis for the dynamics and time responses of the dipoles in pulsed and time-varying electric fields. This treatment will directly lead to the nature of dielectric spectroscopy.

Normal dispersion is characterized as frequency responses in which the dielectric constant increases with increasing frequency. This is typical of non-interactive gases and higher optical frequency regions, i.e. the refractive index, for polar and nonpolar liquids where induced polarizability is in effect. Normal dispersion is attributed to resonance effects as described by quantum mechanics or classically via the forced harmonic or mechanical oscillator as set forth by Cauchy in the 1830's [Prock, 1962 #255].

Anomalous dispersion was first observed by Drude [Drude, 1897 #256] in1897, in which the dielectric constant was measured against the frequency of a standing wave with liquid immersed wires. Anomalous dispersion is characterized as those frequency responses in which the dielectric constant decreases with increasing frequency. This is typical of the microwave, radio, and sub-radio frequency regions for polar liquids where orientational polarizability is in effect.

Takashima [Takashima, 1989 #224] provides the most direct treatment of empirical observables via modern techniques and their fundamental properties. Eq. T15 shows the total polarizability is the sum of the induced and orientational polarizabilities where the total and induced polarizabilities are given by Eq. T11, or

$$\vec{P}_m = \varepsilon_0(\varepsilon_s - 1)\vec{E}$$
$$\vec{P}_d = \varepsilon_0(\varepsilon_\infty - 1)\vec{E}$$

(eq. T25)

where $\varepsilon_s = \kappa_s$, the relative permittivity in a static electric field and $\varepsilon_\infty = \kappa_\infty$, the relative permittivity in a frequency range for the induced polarizability, which must greatly exceed that of orientational polarizability, P_μ.

If an electric field in the shape of a long square pulse is introduced into a sample, the induced polarizabilities, electronic and atomic, will instantly respond to the field. The orientational polarizability will, however, require time to accumulate coherent dipoles with the imposed electric field. This time is characterized by a first-order differential as given by

$$\frac{dP_\mu(t)}{dt} = \frac{1}{\tau}\left(P_\mu - P_\mu(t)\right)$$

(eq. T26)

where τ is the relaxation time and $1/\tau$ is the rate constant.

Debye [Debye, 1929 #183] describes anomalous dispersion to a classical relaxation process in which the demarcation between the high and low dielectric transition occurs at an angular frequency, ω_{tr}, of the imposed electric field by the equation

$$\omega_{tr}\tau = 1$$

(eq. T27)

where τ is the time of the relaxation of the liquid, or more appropriately, τ is the time required for any coherent dipoles to return to a random rotational orientation after the applied electric field is removed.

Assuming the initial value of $P_\mu(t)$ is zero, the solution of Eq. T26 is

$$P_\mu(t) = P_\mu\left(1 - e^{-t/\tau}\right)$$

(eq. T28)

for the coherence of the dipoles to exponentially increase to an increased electric field and similarly

$$P_\mu(t) = P_\mu e^{-t/\tau}$$

(eq. T29)

for the coherent dipoles to exponentially decrease back to a random orientation upon a decrease or removal of the electric field.

A monochromatic sinusoidally changing electric field can be expressed in complex notation as

$$\hat{E} = E_0 e^{i\omega t}$$

(eq. T30)

where ω is the angular frequency given by $\omega = 2\pi f$, where f is the frequency, and E_0 is the maximum amplitude of the electric field. In like manner the electric displacement can be defined as

$$\hat{D} = D_0 e^{i(\omega t - \delta)}$$

(eq. T31)

where δ is the phase shift between the electric field E and the electric displacement D. The polarizability is thus embedded within the phase shift by comparison with Eq. T01. The dielectric constant is the ratio of the electric field E and the displacement D, therefore

$$\hat{\varepsilon} = |\varepsilon| e^{-i\delta}$$

(eq. T32)

where $|\varepsilon| = D_0/E_0$ and by reconciling the real and imaginary components gives

$$\hat{\varepsilon} = |\varepsilon|\cos\delta - i|\varepsilon|\sin\delta$$

or

$$\hat{\varepsilon} = \varepsilon_x - i\varepsilon_y$$

(eq. T33)

therefore the "dielectric constant" or the "relative permittivity" usually means the real part ε_x and ε_y is often known as the dielectric loss. The dielectric loss is absorption of the energy from the applied electric field and dissipation of that energy into the surrounding solvent, usually by thermal mechanisms.

Using the above and Eq. T25 yields the complex orientational polarizability as

$$\hat{P}_\mu = \varepsilon_0(\varepsilon_s - \varepsilon_\infty)\hat{E}$$

(eq. T34)

Substituting Eq. T30 into the latter Eq. T34 and that into Eq. T26 and then solving the differential equation yields

$$\hat{P}_\mu(t) = Ce^{-t/\tau} + \varepsilon_0\left(\frac{\varepsilon_s - \varepsilon_\infty}{1 + i\omega\tau}\right)E_0 e^{i\omega t}$$

(eq. T35)

where the first term is a transient term and will diminish to zero for a steady state solution, therefore it is ignored. The complex orientational polarizability will be the sum of two terms or

$$\hat{P}_\mu = P_d(0) + \hat{P}_\mu(t)$$

$$\hat{P}_\mu = \varepsilon_0\left[(\varepsilon_\infty - 1) + \frac{\varepsilon_s - \varepsilon_\infty}{1 + i\omega\tau}\right]E_0 e^{i\omega t}$$

(eq. T36)

Substituting the latter polarization into Eq. T01 will yield the electric displacement

$$\hat{D} = \varepsilon_0\left[\varepsilon_\infty + \frac{\varepsilon_s - \varepsilon_\infty}{1 + i\omega\tau}\right]E_0 e^{i\omega t}$$

(eq. T37)

and since Eq. T01 also states $D = \varepsilon E$ and Eq. T11 states that $\varepsilon_r = \varepsilon/\varepsilon_0$, then the complex relative permittivity is

$$\hat{\varepsilon} = \varepsilon_\infty + \frac{\varepsilon_s - \varepsilon_\infty}{1 + i\omega\tau}$$

$$\hat{\varepsilon} = \varepsilon_\infty + \frac{\varepsilon_s - \varepsilon_\infty}{1 + (\omega\tau)^2} - i\left(\frac{(\varepsilon_s - \varepsilon_\infty)(\omega\tau)}{1 + (\omega\tau)^2}\right)$$

(eq. T38)

which is known as the Debye-Drude dispersion relation [Debye, 1929 #183]. The second line separates the real and imaginary components of the complex permittivity by taking the complex conjugate of the first line where finally by using Eq. T33 the separated components are

$$\varepsilon_x = \varepsilon_\infty + \frac{\varepsilon_s - \varepsilon_\infty}{1 + (\omega\tau)^2}$$

$$\varepsilon_y = \frac{(\varepsilon_s - \varepsilon_\infty)(\omega\tau)}{1 + (\omega\tau)^2}$$

(eq. T39)

Normalizing and plotting the latter complex dielectrics yields

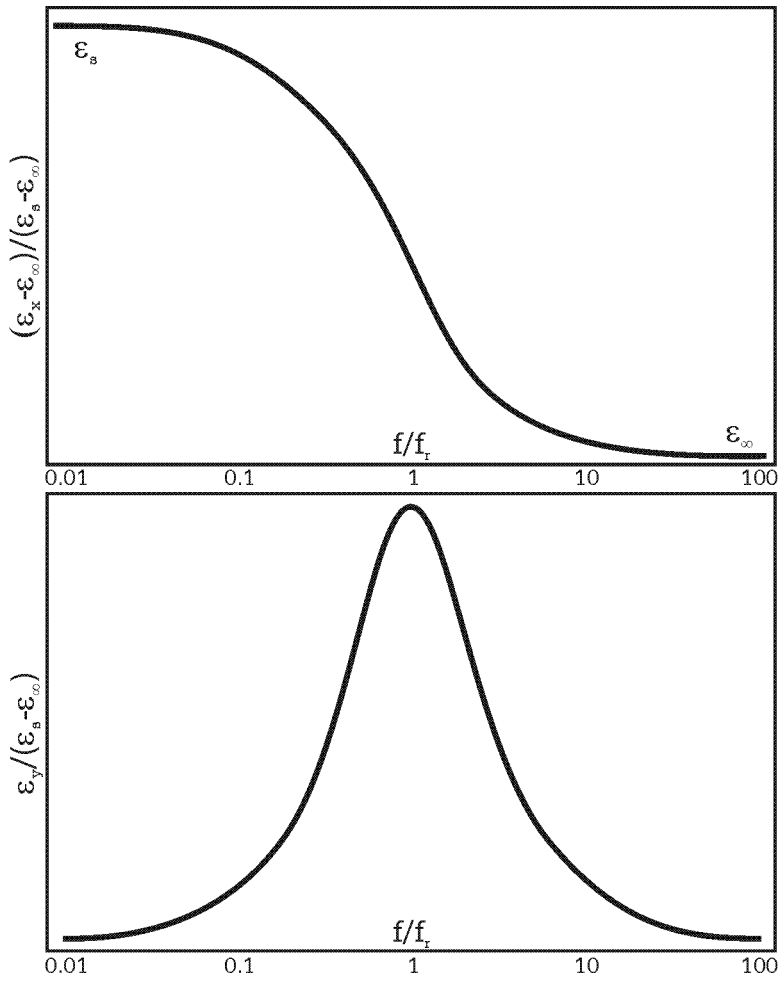

(fig. T01)

The top plot is that of the real permittivity, or the "dielectric constant", and the bottom plot of the imaginary component of the permittivity. The real and imaginary permittivity are simultaneously measured by modern detectors, such as a vector voltmeter, phase-locked-loop, lock-in amplifier, or phase discriminator.

The generally accepted interpretation of the complex permittivity is that the permanent dipole is coherent and can follow the applied electric field below the transition frequency. As the frequency approaches the transition, or $1/\tau$, then the dipole is approaching a maximum rotational velocity, which is visualized above with $f < f_r$, or $f/f_r < 1$. As the incident frequency f approaches the transition frequency f_r of the dipole then the increased rotational velocity causes the dipole to absorb greater electrical energy from the applied electric field and thus dissipate more of the absorbed energy into the surrounding solvent. The dissipation would be in the form of friction with the local solvent molecules, thus an electrical to thermal conversion occurs around the transition frequency. As the incident frequency exceeds the transition frequency, or $f > f_r$, or $f/f_r > 1$, then the dipole can no longer maintain its coherence with the applied field and thus more dipoles return to a random orientation. Since the

majority or all of the dipoles are in the random orientation, the polarization due to orientation is not effectual and thus a drop in the real permittivity is expressed.

Debye [Debye, 1929 #183] considered the dielectric loss, the imaginary component of the permittivity, as a frictional loss of the molecular permanent dipoles with the surrounding solvent molecules. The solution of Debye's treatment can simply be expressed as

$$\tau_{\text{int rinsic}} = \frac{4\pi a^3 \eta}{kT}$$

(eq. T40)

where a is the radius of a perfectly spherical molecular dipole, η is the viscosity of the solution, k is Boltzmann's constant, and T is the temperature. Therefore, the rotary diffusion of the dipole, which is characterized by the intrinsic relaxation time $\tau_{\text{intrinsic}}$, is strongly affected by its environment. This environment is based on the viscosity and temperature of the solution, and the molecular volume of the dipole itself. The molecular surface area, obviously, is a direct relationship of its radius, a, and thus its volume, a^3, therefore, larger molecules maintain a higher intrinsic relaxation time due to greater friction, and thus viscosity, with its solvent.

The intrinsic relaxation $\tau_{\text{intrinsic}}$ is not the same as τ in Eq. T39, for τ does not allow for the viscosity of the medium. It has been proven, however, that the two are related via

$$\tau_{\text{int rinsic}} = \tau \frac{\varepsilon_\infty + 2}{\varepsilon_s + 2}$$

(eq. T41)

as provided by Takashima [Takashima, 1989 #224]. It is apparent that the above treatment of τ and $\tau_{\text{intrinsic}}$ involves assumptions on the shape of the molecular dipole, that being of spherical symmetry, however, most globular proteins are of nearly spherical symmetry. Therefore, Debye's assumptions of spherical symmetry is a good approximation for studies of globular proteins.

In summary, an electric field imposed on a real sample of peptides or proteins will exhibit a complex permittivity, which is a directly measurable quantity. The complex permittivity is a function of the mass, volume, and strength of the permanent dipole moment of the peptides or proteins themselves. It is also a function of the environment of the peptides or proteins, the solution, its viscous drag, intermolecular electrical bonding, electrical shielding, and temperature, owing to the disorder of the solution itself and its interactions with the peptides or proteins. The measurement of the complex permittivity is the technique employed in dielectric spectroscopy.

Biological Molecules

Biological molecules include all of the compounds, material, and stuff found in living systems. The biological molecules include water, salts, vitamins, minerals, lipids or fats, proteins, ribonucleic acid (RNA), and deoxyribonucleic acid (DNA). Water is commonly known to exist in life and DNA frequents our mass media for the criminal system. Most living systems are composed of approximately 70% water, 25% protein, and less than 0.1% DNA.

Protein is the foundation of life. It forms the structure of and monitors, mediates, and catalyzes all chemical reactions within a living system. Protein is the "nuts and bolts" of life and a full understanding of protein will benefit all aspects of life, our ecosystem, our health and its management, and even our future technologies. It is this motivating factor that inspires the PDP towards the detailed study of proteins. This section will focus primarily on proteins and water.

Water

Water forms the foundation of all living systems and it is the primary reason for life on this planet. Water is a very simple molecule that happens to exhibit complex, and sometimes bewildering, characteristics. For instance, the density of most solids is greater than that of the respective liquid, thus the solid will sink in its own liquid. Ice, however, is less dense than water as exhibited by ice floating on water.

The structure of water is

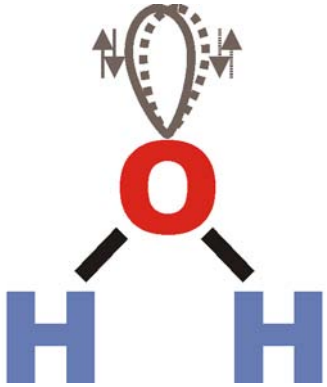

(fig. B01)

where the HOH angle is 104.474°, as measured in the gas phase by infrared spectroscopy [Eisenberg, 1969 #259]. Under molecular orbital theory, the oxygen is sp^3 hybridized which implies a tetrahedral orbital configuration. The unperturbed angle of adjacent tetrahedral orbitals is 109.5°, however, water contains two lone pair of electrons which perturb the tetrahedral configuration and compress the HOH angle down to 104.474°. The lone pair of electrons are centered above the oxygen, in and out of the 2D page, and the perturbation is based on the electrostatic repulsion of the lone pairs with the σ-OH bonds.

It is the structure of water that makes it so unique and perplexing. For instance, the compressed HOH angle causes water to expand upon freezing and thus ice is less dense than water. It is also the reason for water generally accepted as the "universal" solvent and excellent thermal stabilizer. Both of these properties are because of the HOH angle, the two lone pairs of electrons, and the partial charges derived from the nonlinearity of the molecule.

Hydrogen bonds are a weak intermolecular bond between the partially positive hydrogen and the partially negative oxygen of a neighboring water molecule, or

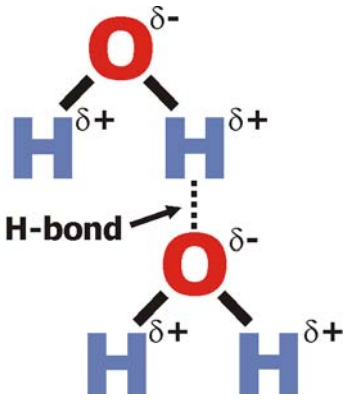

(fig. B02)

Hydrogen bonds possess and energy of 4 to 12 kcal/mol and form throughout the liquid completing a complex lattice of highly dynamic semi-structured crystals, known as flickering clusters, imparting greater thermal stability within the liquid.

Water can also form hydrogen bonds with other molecules. This is found in proteins, where bound water layers have been observed using X-ray crystallography, NMR, and dielectric spectroscopy. It is believed that the bound water layers, both internally to and externally upon the surface of the protein, aid the protein in solvation, motion, catalysis, and charge transfer, distribution, and balancing. The bound water of proteins will be an important factor in the study of the PDP.

Water will naturally dissociate, in which the products of the dissociation are a hydronium, or a proton, and hydroxide ion. The reversible reaction is

$$H_2O \Leftrightarrow H^+ + OH^-$$

(eq. B01)

Water will not conduct electricity, however, water's ions, the hydronium and hydroxide, will carry an electric current because of their charge. Careful conductivity measurements on pure water reveal an ion product k_w of

$$k_w = 10^{-14} = [H_2O]k_{eq} = [H^+][OH^-]$$

(eq. B02)

and the concentrations of both ions will be equal in pure water. The concentration of hydronium or hydroxide would be 10^{-7} M, or a pH of 7, in pure water.

The dissociation of water must be accounted for in dielectric measurements because the conductivity, or its inverse, the resistivity, of the hydronium or hydroxide ions will cause a decrease in the capacitance. Or, in other words, the real component of the complex impedance will be increased as a function of increased conductance and thus shift the complex current measurements from the imaginary capacitance measurements to the real conductance.

Electrical Properties of Water

As shown in Fig. B02, the partial positive charges on the hydrogen and the partial negative charges on the oxygen form the basis of a permanent dipole moment. The strength of the dipole is greatly enhanced by the presence of the two electron lone pairs in the sp^3 hybridized oxygen for they compress the HOH angle and provide additional negative charge above the oxygen.

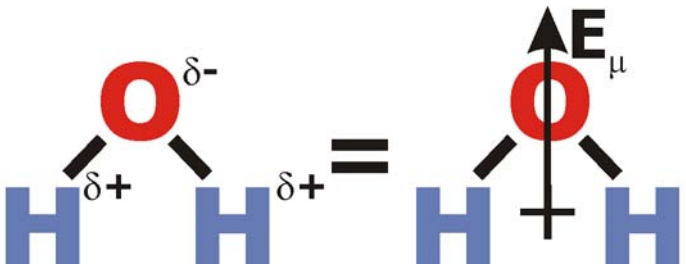

(fig. B03)

The strong charge separation creates a net and permanent dipole moment which possess its own electric field, E_μ. The strength of the dipole moment of steam is 1.84 ± 0.02 D (1.84×10^{-18} e.s.u.) [Sanger, 1928 #258], [Smyth, 1955 #260].

Electrostatic theory states that water's dipole moment will align in the presence of an applied electric field. This is proven by pure water having an electric permittivity of approximately 80 at room temperature [Weast, 1982 #257]. The anomalous dispersion of water ranges from a permittivity of 88.3 at 0.5769 GHz and decreases down to a permittivity of 4.23 at 890 GHz with the resulting relaxation time on the order of 10 ps, or 16 GHz [Takashima, 1989 #224]. At 20° C, the dispersion curve for water is nearly constant from static to 1 GHz, exhibiting only a 0.3 % decrease of ε_s at 1 GHz [Grant, 1978 #248]. Therefore, a dielectric study under 1 GHz, of biological molecules in aqueous solution will require measuring a relatively small obscure biological dielectric signal through the rather large dielectric signal of bulk water.

Bound water, i.e. the water weakly bound externally to or embedded within a protein, would have a greater relaxation time than that of free water because of the stronger forces linking the water to the protein. Bound water would be more ice-like than free water [Grant, 1978 #248]. Hence, a greater relaxation time would decrease the frequency of the observed dispersion.

In addition to the relaxation time, the static permittivity, ε_s, of ice is nearly equal that of free water, therefore that of bound water would be within the range of 80 to 100. The infinite-frequency permittivity, ε_∞, of ice is 3.2 and that of water is 4 to 4.5, in which the anticipated value for bound water would similarity lie within that range. Therefore, it is reasonable to conclude that the dielectric constants of bound water lie within the regions of ice and water with a shifting of the relaxation time for bound water.

Amino Acids

Proteins are extremely large complex molecules. For instance, a very small protein can have many thousands of atoms. Thankfully, proteins are composed of subunits called amino acids. There are only twenty different amino acids found in all living systems in which they all have the same basic structure, as follows

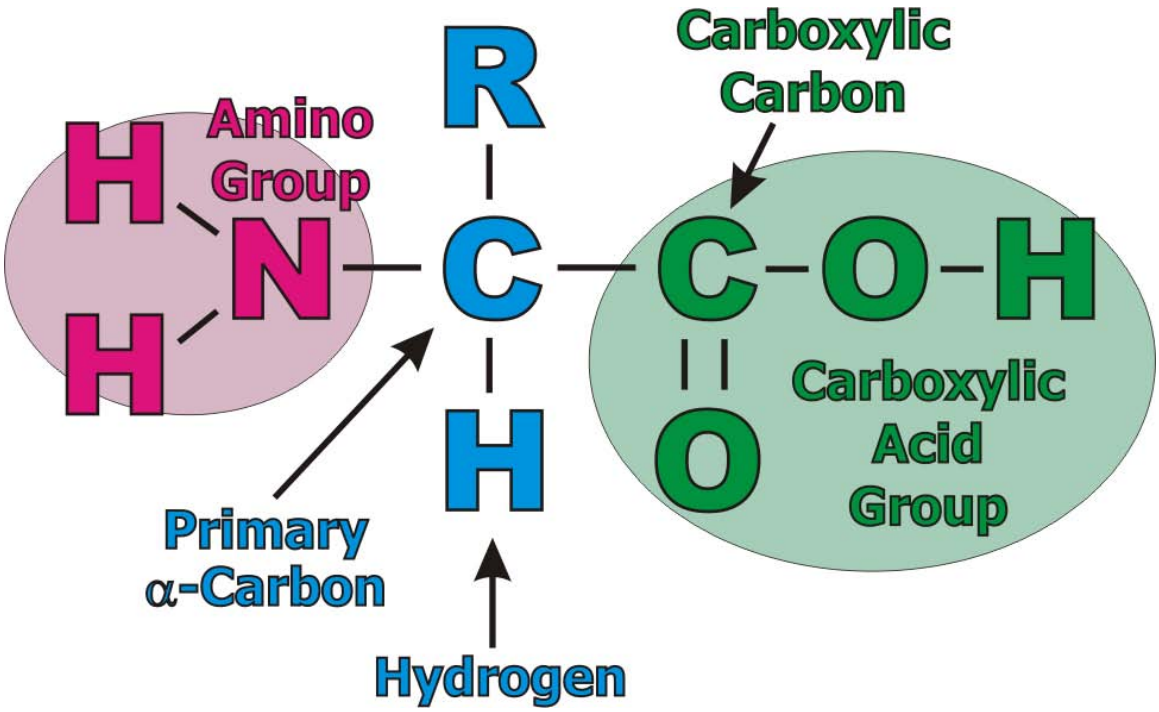

(fig. B04)

The Hydrogen bonded to the primary carbon is always Hydrogen. This is important for the polarity and hydrophobicity of the overall protein and in how a protein will eventually fold in on itself. The primary carbon is also known as the α-carbon (alpha-carbon).

The term amino acid comes from the amino functional group on the left and the carboxylic acid group on the right. It is noteworthy to state that the amino group is inherently a base and the carboxylic acid group is an acid, therefore, amino acids, and thus proteins, are both acids and bases. Molecules that are both acids and bases are known as amphoteric and possess the quality of being good buffers. Buffers have the ability to stabilize the pH of a solution within a specific pH range.

All twenty amino acids are the same except for the R group. The simplest R group is a Hydrogen and equates to the amino acid Glycine. The most complex amino acid is Tryptophan where the R group is a complex Nitrogen-containing double ring structure known as an indole group.

The distinguishing R group imparts on the amino acid its physical and chemical properties. Some R groups are very polar and thus readily dissolve in water, others are nonpolar and thus hydrophobic. The hydrophobicity of the R group is important for it will determine the shape and function of the protein.

Proteins are formed by simply bonding the amino group of one amino acid to the carboxylic acid group of another amino acid in a dehydration reaction where water is given off.

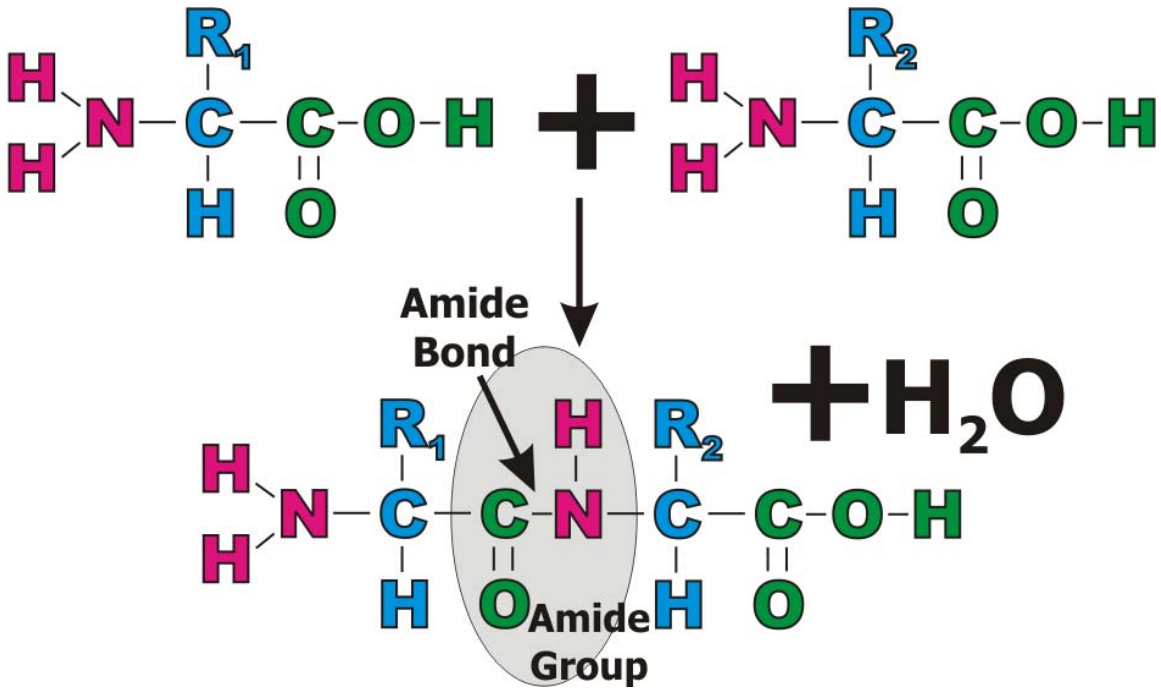

(fig. B05)

Two amino acids bonded together are a dipeptide. Polypeptides are proteins or peptides with many amino acids. Most functional proteins require at least thirty amino acids in length. Insulin has 51 amino acids.

Electrical Properties of Amino Acids and Peptides

The nitrogen in the amino functional group has a lower electronegativity then its σ-bonded hydrogens, therefore the nitrogen will exhibit a partial positive charge. The carbonyl oxygen on the carboxylic carbon will be strongly electronegative because of the additional π-bonding. This will create a strong negative charge on the carbonyl oxygen. The presence of the positive charge on the amino nitrogen and the negative charge on the carbonyl oxygen, separated by an atomic distance, is a permanent dipole moment. Therefore, free amino acids in solution will exhibit an orientational dielectric response. Depending on the R group of the amino acid, it can also have an additional additive or subtractive effect

on the net permanent dipole moment. Essentially, those amino acids with polar R groups will exhibit different dielectric responses as opposed to nonpolar R groups.

Proteins

Proteins are a class of biomolecules that perform two primary functions in all living cells. The first function is structural. Proteins form the structural basis of an organism. For instance, skin, bone, hair, and finger nails are pure forms of protein. Of all the protein in mammals, thirty percent is collagen. It is a sheet-like protein in your skin that keeps it tight and young looking. As we age the bonds in the collagen weaken and the face begins to age. Tendons, which connect the muscles to the bones, are also composed of collagen, and as in the face, mobility and flexiblity decreases with age.

The second function of proteins is catalytic, or they facilitate chemical reactions. Proteins that act as catalysts are called enzymes. Insulin is an enzyme that maintains the level of glucose in your blood stream. Diabetes is the desease when the level of insulin or its enzymatic efficiency is decreased.

The Protein Data Bank (PDB) is a world-wide despository of protein structures that be accessed via the internet, or http://www.rcsb.org. The PDB is a searchable database of X-ray crystallographic and NMR-based 3D atomic coordinates of proteins and stored in text files called PDB can be accessed

Myoglobin and hemoglobin will be used as examples to explain the concepts of protein structure.

Although extremely large and complex, a protein's structure can be broken down into four stages of complexity. The first is the primary structure in which the exact amino acid length and linear sequence of amino acids determine the protein.

The secondary structure is the initial folding of the protein upon itself. The length and sequence of the primary structure along with the hydrophobicity of the R groups determine how the initially linear backbone of the protein will fold in on itself. The α-helix, the β-sheet, and the random coil form the three secondary configurations of folding and twisting. Essentially, hydrophilic R groups will face outward on the protein and hydrophobic R groups will form a tight inner core. This is due to the water environment of the cell in which proteins reside.

Tertiary structure occurs when certain R groups physically bond with other R groups. The primary bond would be a disulfide bride between the two sulfur containing amino acids, cysteine and methionine. These chemical bonds formalize the folding of the protein into a more rigid and permanent structure.

Quaternary structure will only occur when multiple polypeptide chains bond to form an even larger functional protein. Not all polypeptides require bonding to other peptides to be a functional protein.

The four stages of protein structure are shown below.

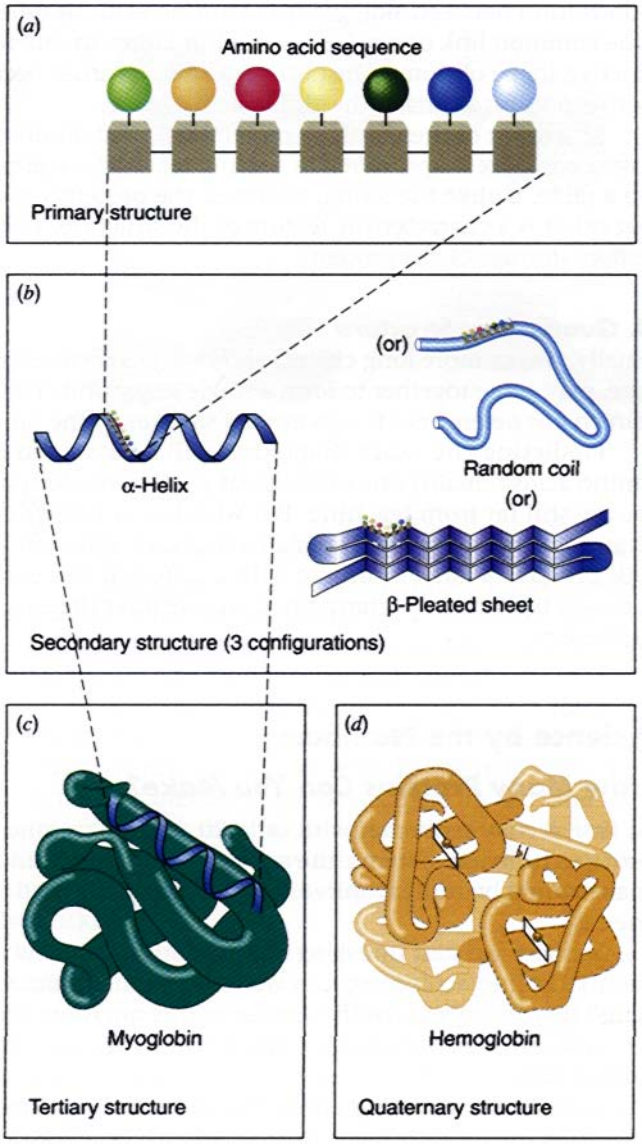

Myoglobin and Hemoglobin

Myoglobin and Hemoglobin are molecules that transport Oxygen from the lungs, upon inhalation, to the tissues through the blood stream. When the oxygen is released from the molecule, it then accepts Carbon dioxide waste from the cells, delivers it back to the lungs in which it is released upon exhalation. Myoglobin is usually found in lesser evolved animals, such as fish, and Hemoglobin is found in mammals and primates. Both are responsible for making blood the color red.

The cells use the Oxygen in cellular respiration to metabolize glucose and derive energy or ATP through the oxidation of that glucose. The six carbons in each glucose are oxidized to the point of producing Carbon dioxide, which is then considered waste by the cell and expelled. Myoglobin and Hemoglobin ensure that each of the cells in the organism have an ample supply of oxygen and properly remove the Carbon dioxide waste.

Myoglobin is the more simple of the two molecules. It primary structure consists of a single polypeptide chain of 153 amino acids in length, as shown

H_2N – Val – Leu – Ser – Glu – Gly – Glu – Trp – Gln – Leu – Val – Leu – His – Val – Tyr – Ala – Lys – Val –
Glu – Ala – Asp – Val – Ala – Gly – His – Gly – Gln – Asp – Ile – Leu – Ile – Arg – Leu – Phe – Lys –
Ser – His – Pro – Glu – Thr – Leu – Glu – Lys – Phe – Asp – Arg – Phe – Lys – His – Leu – Lys – Thr –
Glu – Ala – Glu – Met – Lys – Ala – Ser – Glu – Asp – Leu – Lys – Gly – His – His – Glu – Ala – Glu –
Leu – Thr – Ala – Leu – Gly – Ala – Ile – Leu – Lys – Lys – Gly – His – His – Glu – Ala – Glu –
Leu – Lys – Pro – Leu – Ala – Gln – Ser – His – Ala – Thr – Lys – His – Lys – Ile – Pro – Ile – Lys –
Tyr – Leu – Glu – Phe – Ile – Ser – Glu – Ala – Ile – Ile – His – Val – Leu – His – Ser – Arg – His –
Pro – Gly – Asn – Phe – Gly – Ala – Asp – Ala – Gln – Gly – Ala – Met – Asn – Lys – Ala – Leu – Glu –
Leu – Phe – Arg – Lys – Asp – Ile – Ala – Ala – Lys – Tyr – Lys – Glu – Leu – Gly – Tyr – Gln – Gly – COOH

The secondary structure contains eight sublengths of α-helicies with a random coil between each α-helix.

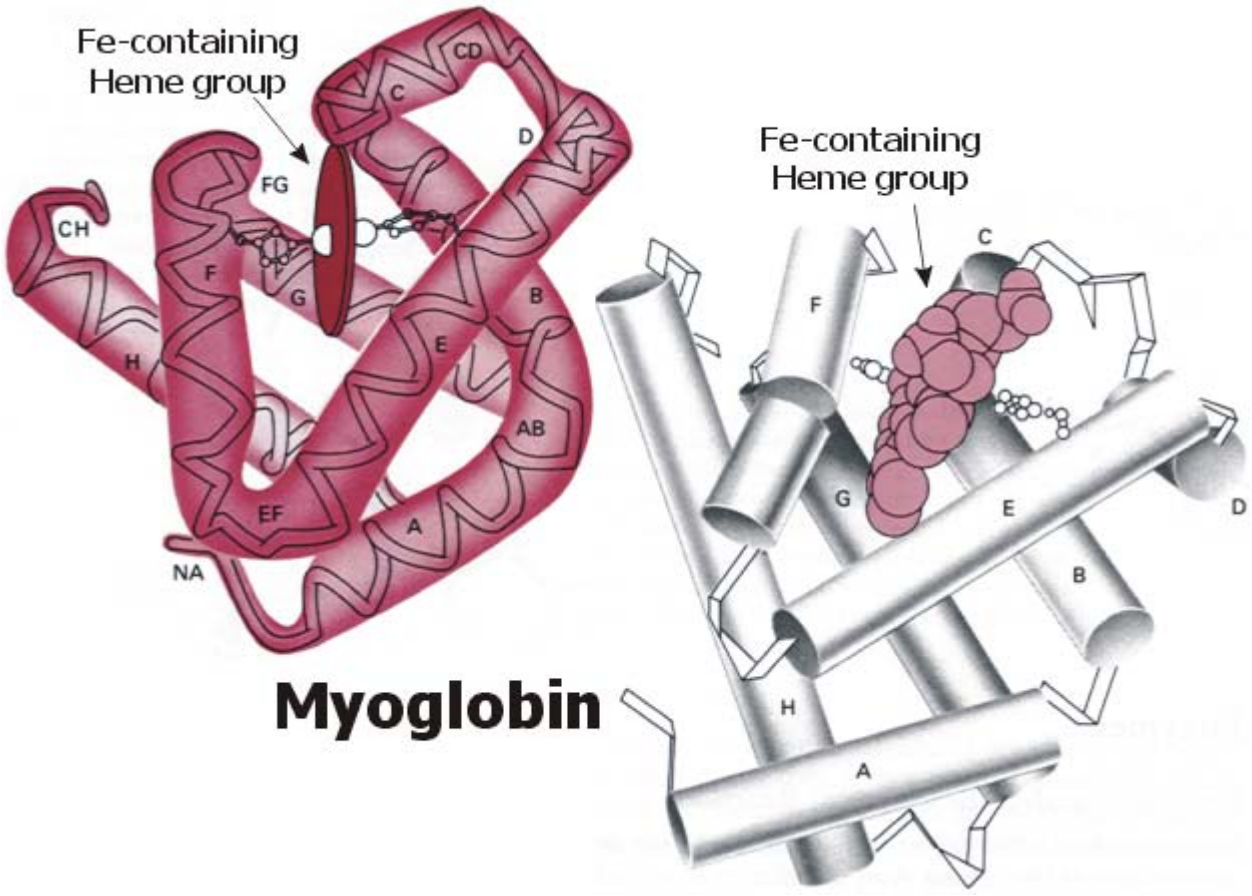

where the above diagram is actually two different concept drawings of the same single Myoglobin molecule. Notice how the α-helicies and tight turns are similar between both renderings.

Anemia is the lack of red blood cells and more specifically a lack of Myoglobin or Hemoglobin in the blood to carry enough Oxygen to the cells or remove the CO_2 waste. Increasing the intake of Iron (Fe) will often stimulate the production of Myoglobin or Hemoglobin and thus increase the concentration of red blood cells in the stream. Iron is an integral and necessary part of the Myoglobin and Hemoglobin molecule. It forms the center of the heme group which is embedded in the center of the polypeptide chain, as shown above. The chemical structure of the heme is as follows

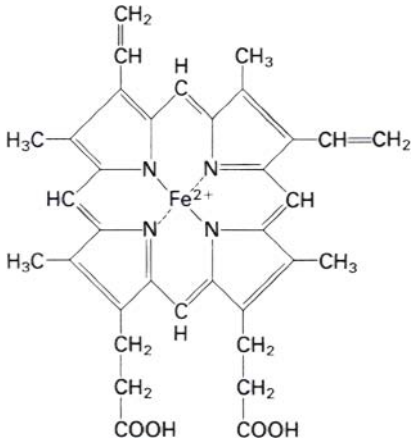

When Oxygen is bound to the Fe atom it causes the heme ring structure to pucker. This puckering causes the peptide portion of Myoglobin to break any bonds with the CO_2 waste the molecule is carrying back from the cells. The CO_2 is actually carried on the N-terminal end of the peptide, or at the end of the A α-helix in the above Myoglobin diagram. Therefore, Myoglobin and Hemoglobin not only act as a dual transport system, they do it efficiently because the molecules will never carry O_2 and CO_2 at the same time.

Hemoglobin performs the same job as Myoglobin. It is structurally a bit different then Myoglobin in that Hemoglobin requires four polypeptide chains to bond in a full quaternary structure. This four times more massive molecule is much more efficient at performing its duties then Myoglobin.

The primary structure of Hemoglobin is slightly modified to account for the larger more complex molecule. Two of the four Hemoglobin polypeptides are known as the α-chains, the other two are the β-chains. The α-chain is 141 amino acids in length and the β-chain is 146 amino acids long. The primary structure is shown below in which the identical regions are shown in red.

The secondary and quaternary structure can be seen in the following diagram

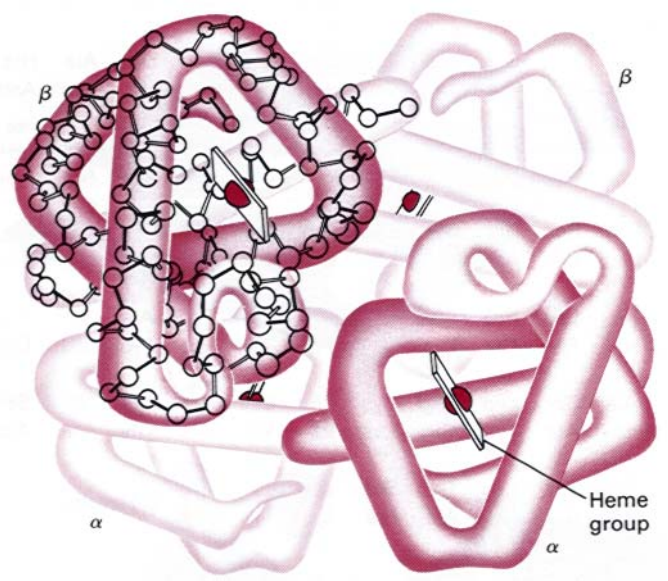

When we inhale, the blood in our lungs has a very high concentration of O_2. This high concentration of O_2 in the blood forces bonding of O_2 with the heme Fe atom. The puckering of the heme group occurs. Any CO_2 still bound to the N-terminal end of the polypeptide will be released from the molecule and then exhaled. Hemoglobin is more efficient then Myoglobin because after the first O_2 molecule bonds to the heme Fe atom in Hemoglobin, it not only induces the release of CO_2, but also sends a signal to the other three polypeptides. This chain reaction will stimulate them to bind much more easily to other free O_2 molecules. Myoglobin acts independently and does not have this interpeptide communication as does Hemoglobin, for it can work in concert as a massive four polypeptide molecule.

When the O_2-rich Hemoglobin arrives to an area with a very low concentration of O_2 and a high concentration of CO_2, the Hemoglobin is stimulated to release its O_2 cargo and bond to CO_2. The same interpeptide stimulation occurs, but in the reverse. Once the first O_2 molecules is released, it stimulates the other three to release O_2 that much easier and pickup CO_2.

Electrical Properties of Proteins

The driving force for the formation of secondary structure in peptides and proteins, herein known simply as proteins, is steric hindrance and reduction of charge caused by inherent dipole moments. The typical amide or peptide bond carries a dipole moment of 3.7 Debyes ($D = 10^{-18}$ esu cm) [Cantor, 1980 #266]. The charge of an electron is 4.8 D, therefore in comparison, the amide bond imposes a large charge buildup and thus the primary structure of a protein contains a charge of the product of 3.7 D by its amino acid length. The reduction of the charge buildup due to the amide bond dipoles will dominate the folded secondary structures.

The secondary structure of proteins consist of structural motifs which naturally form to alleviate the inherent charge created by the electrical nature of bonded amino acids, the amide or peptide bond. In the grand scheme of things, these dipole moments are the smallest in scale within a protein, however, the great number of peptide bonds forces the protein to reduce this charge effect by cancellation. The primary structure of the protein will fold within itself to reduce this charge, thus the structural motif is

created. The most prevalent motifs are hairpin turns, random coils, α-helices, and β-sheets, in which the latter two possess the most structure and the greatest reduction of charge due to the peptide bonds.

The structural motifs of α-helices and β-sheets reduce peptide bond charge buildup with the formation of hydrogen bonds. In general, hydrogen bonds between intramolecular residues form from the attraction of the partial negative of the carbonyl oxygen with the partial positive of the amine hydrogen. Or, the formation of hydrogen bonds within the secondary structure causes a decrease of the overall charge buildup within the protein. The decrease of such charge reduces the overall energy of the protein and thus energetically stabilizes its overall structure.

The α-helix structural motif will form a hydrogen bond between a carbonyl oxygen and the amino hydrogen of every 4^{th} residue. This imposes a periodicity of 3.6 residues for the α-helix. Although the α-helix greatly reduces the net peptide bond charge, it still possesses an overall permanent dipole moment in the direction of the helical axis. This is because the α-helix has the amide bonds pointing nearly parallel to the helical axis, thus causing the formation of a net dipole moment along the axis of the helix. Therefore, a strong permanent dipole moment exists for α-helix structural motifs that should possess an extremely active dielectric response.

The β-sheet structural motif will also form hydrogen bonds between respective carbonyl oxygen and amino hydrogen to reduce the charge buildup of the peptide bond. β-sheets form parallel and antiparallel sheets in which both forms cause the direction of the amide bond to alternate. This causes an overall cancellation of a net dipole for β-sheet structural motifs and thus a permanent dipole moment of β-sheet would be very small. Although the dielectric response of β-sheets would be smaller than that of α-helices, β-sheets should still possess a dielectric response due to induced polarization effects, such as electronic or atomic polarization. A practical example of this is benzene. Benzene does not possess a permanent dipole moment, however it still posses an induced dipole which is detectable with sensitive instrumentation.

Random coils and hair-pin turns would possess less predictable permanent and induced dipole because of their irregular structure. However, detection of a dielectric response from such structural motifs may provide valuable statistical and environmental data for understanding protein structure and internal dynamics.

The tertiary structure of proteins is founded on the secondary structure of the motifs. The internal hydrophobic cores of globular proteins have been observed as being highly viscous and glass-like. The high viscosity between motifs, or interchains, would greatly increase the relaxation time, and thus lower the observed relaxation frequency within a single protein as compared to that same ideal motif free within aqueous solution [Debye, 1929 #183]. It is for this reason that this proposed project is attempting to detect and characterize the secondary structural motifs at much lower frequencies than previous dielectric work on proteins, which only characterized the net dipole moment of entire proteins in solution.

It is clear that proteins possess a strong electrical nature. The electrical nature derives from the strong electronegative forces of the amide or peptide bond of the primary structure. The secondary structure attempts to alleviate much of the electrical pressure with the conformational reorganization leading to hydrogen bonds. Highly ordered secondary structure lead to structural motifs of α-helices, which

possess a strong permanent dipole moment, and β-sheets, which possess a weak permanent dipole moment but detectable induced dipole moments. Less ordered motifs, such as random coils and hair-pin turns currently have an unpredictable dipole moment, but should provide further insight into the internal nature and dynamics of proteins. It is this electrical nature of proteins that inspires this project to detect and categorize these electrical moments via advanced dielectric spectrometers.

Instrumentation and Experimental

Complex Impedance

An alternating voltage, monochromatic sine waveform, applied to a circuit will create an alternating current (A.C.). This will modify the resistive Ohm's Law to an impedance, or

$$V = IZ$$

(eq. I01)

where Z is the complex, real and imaginary, impedance and replaces the purely real resistance R in Ohm's Law in a static, non-time varying, direct current (D.C.) circuit.

Halliday [Halliday, 2001 #252], Serway [Serway, 2004 #253], and Feynman [Feynman, 1989 #254] discuss the reactance of a capacitor in an A.C. circuit, as shown

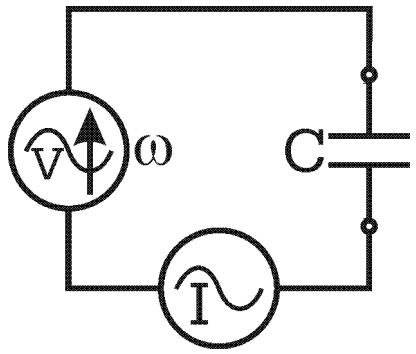

(fig. I01)

where the voltage source V drives the charge Q buildup and decay on the capacitor with capacitance C and the current I is measured with an appropriate A.C. ammeter.

The voltage across the capacitor is given by

$$V = \frac{Q}{C}$$

(eq. I02)

and the current I is the given by the rate of change of the charge within the capacitor, or

$$I = \frac{dQ}{dt}$$

(eq. I03)

and finally the rate of change of the sinusoidally varying voltage can be expressed by

$$\frac{dV}{dt} = i\omega V$$

(eq. I04)

where $i = \sqrt{-1}$ and ω is the angular frequency of the source or $\omega = 2\pi f$. Upon combining the three latter equations derives

$$V = \frac{I}{i\omega C}$$

(eq. I05)

and thus equating the latter with Eq. I01 gives

$$Z_c = \frac{1}{i\omega C} = -\frac{i}{\omega C}$$

(eq. I06)

where the complex impedance for a capacitor is also known as the capacitive reactance Z_c. The purely imaginary capacitive reactance in an A.C. driven circuit implies a phase difference between the applied voltage and the measured current. An ideal or perfect capacitor, therefore, will produce a current that leads by 90° as compared to the applied sine wave voltage, where leading implies a -90° phase difference, as shown in Eq. I06 by the -i.

A perfectly resistive A.C. circuit will exhibit a zero phase difference between the source voltage and the measured current thus leading to a purely real reactance of

$$Z_r = R$$

(eq. I07)

in which is purely resistive A.C. circuit is not frequency dependent.

Thusfar, the discussion has only considered ideal capacitors and resistors. A real capacitor will always exhibit some loss. The loss of a capacitor has been traditionally treated as a resistive factor providing the impedance of a real capacitor as

$$Z = Z_r + Z_c = R - \frac{i}{\omega C} = R - \frac{i}{2\pi f C}$$

(eq. I08)

A capacitor allows the propagation of an electric field through a dielectric medium. The ability of the capacitor to hold that charge and maintain a constant electric field between the conductive plates is expressed in the latter imaginary term, hence an ideal capacitor. However, a real capacitor is constructed with a dielectric material between the plates in which the induced and orientational polarizabilities of the material will couple with the applied electric field. The coupling may cause the material to absorb some of the energy from the applied electric field and thus dissipate the absorbed energy into other forms of energy, usually thermal.

For example, a polar liquid is the dielectric material which will couple to the electric field through orientational polarization. Such coupled molecules will rotate to maintain coherence with the field, and in so doing, loose energy to the bulk medium through intermolecular friction with its locally surrounding solvent molecules. This is the conversion of the absorbed field energy with loss to thermal energy, in which the loss is detected as the real component of the complex impedance. Vector voltmeters, phase discriminators, and modern lock-in amplifiers will simultaneously measure both the real and imaginary components of the complex impedance, therefore providing the relative degree of capacitance, or charge storage, and resistance, or energetic loss, for a particular dielectric medium and associated real capacitor.

Measuring the complex impedance or V/I provides a direct correlation to the resistance and capacitance, via the reactance, of the cell. It is also a common practice to measure the complex admittance which is the measurement of I/V, or simply the inverse of the impedance. This leads to the conductance and susceptance of the cell, in which both are inverses of resistance and the capacitive reactance, respectively.

Solving Eq. I08 for the complex capacitance C will yield

$$C^*(\omega) = \frac{VI'' + i\left(RI^2 - VI'\right)}{\omega\left(\left(RI' - V\right)^2 + \left(RI''\right)^2\right)} \qquad \text{(eq. I09)}$$

where I_x is the real component of the measured current, I_y is the respective imaginary component, and $I^2 = I'^2 + I''^2$. Each term in the numerator is a power term, where $P = IV = I^2R$, and the denominator is the angular frequency, ω, times the square of the impedance, Z^2.

Empirical results of the measured capacitance reveal that the measured capacitance C has a more complicated dependence on frequency then a simple $1/\omega$ relationship. In fact, the response of the bulk material, and that of the underlying intra and intermolecular potentials, to the applied electric field are expressed through the measured complex current. In fact

$$I^* = I'(\omega) - iI''(\omega)$$
$$R = R'(\omega) \qquad \text{(eq. I10)}$$

where the resistive component is implied through the real component of the current, I'. Therefore, the direct measurement of the complex current will lend itself to the resistance and capacitance of a real

capacitor/condenser. The design of such a capacitor, or sample holder, with a liquid dielectric material between the conductive metal plates will measure the direct measurement of the relative permittivity at a particular imposed frequency or

$$\varepsilon^*(\omega) = \frac{C^*(\omega)}{C_0^*(\omega)} = \frac{Z_0^*}{Z^*} = \varepsilon_x - i\varepsilon_y$$

(eq. I11)

or the relative permittivity, ε, is the measured capacitance C of the dielectric medium at a particular frequency is divided by the measured capacitance C_0 of the same condenser/capacitor under vacuum.

Since the ultimate goal of the PDP is to measure the complex dielectric response of peptides and proteins, the complex permittivity is given by

$$\varepsilon^* = \frac{Z_r^*}{Z_s^*}$$

(eq. I12)

where Z_r is the impedance of the reference or blank cell, such as water, and the Z_s is that of the sample, such as a protein in water.

Substituting Equation I01 into the latter will yield

$$\boldsymbol{\varepsilon}^* = \frac{Z_r^*}{Z_s^*} = \frac{Y_s^*}{Y_r^*} = \frac{V_r}{I_r^*}\left(\frac{I_s^*}{V_s}\right) = \frac{V_r}{V_s}\left(\frac{I_s^*}{I_r^*}\right)$$

(eq. I13)

where the sample and reference are measured at a single specific frequency ω.

The latter currents are measured relative to the applied voltages, therefore the voltages are expressed with only a real component and the expression of the currents will be complex. This leads to the complex permittivity with separation of the components as

$$\varepsilon' = \frac{V_r}{V_s}\left(\frac{I_s' I_r' + I_s'' I_r''}{I_r'^2 + I_r''^2}\right)$$

$$\varepsilon'' = \frac{V_r}{V_s}\left(\frac{I_s' I_r'' - I_r' I_s''}{I_r'^2 + I_r''^2}\right)$$

(eq. I14)

The measurement of the complex current of the sample, along with comparison to the reference, will lead to the complex permittivity of the sample. This will ensure that the capacitor geometry and most fringe effects will be nulled from the permittivity of the sample. The measured complex permittivity then leads to the anomalous dispersion and absorption as discussed in the Theoretical section, and finally to the orientational polarizability and solvent effects of the dipole within the same section.

Phase I Dielectric Spectrometer

Traditional impedance/dielectric spectrometers were based on bridge circuits, such as the deSauty and Schering bridge, to null out noise and measure the complex capacitance of a sample cell. Although bridge circuits perform well, they can have a complicated circuit design and have a limited frequency range. Bridge circuits require a balancing method to null the detected complex current across the bridge. The method of balancing requires that the bridge be rebalanced for each change in frequency, hence the mass-produced auto-balancing bridge, as that of Agilent Technologies.

Traditional spectrometers have measured the permittivity using two techniques. The first method introduced a pulse, of arbitrary shape, into the sample and performed a fast-fourier transform (FFT) on the signal versus the original pulse. This technique is analogous to modern infrared (FT-IR) spectrometers and has the advantage of nearly instantaneous measurements and spectral acquisition. Although this procedure has had promise, proper amplification and signal processing, as well as noise effects, have made it impractical for most peptide and protein studies. In the future, we would like to reconsider this method for biopolymer dielectric measurements in our research endeavors.

The second technique imposed a single monochromatic sinuously-varying voltage and detected the response at the imposed frequency. This technique has proven extremely successful because modern op.amps. can be configured for a specific and predetermined frequency range, thus allowing proper calibration, amplification, and characterization within the said frequency range. Additionally, focusing the detector on a single frequency allows the digital-signal processor (DSP) circuits to properly filter any noise inherent to or introduced by the circuit. Essentially, detectors are far more sensitive by focusing on a single sinusoidal frequency.

Overall, the latter method starts a scan at a predetermined frequency and incrementally and discreetly steps through a range of frequencies. The complex current is then measured at each incremental frequency. A computer is used to accumulate the data and plot the respective dielectric spectrum.

Traditional bridge circuits are complicated, especially auto-balancing, and require rebalancing and recalibration at each frequency, therefore bridges will not be used in our research. The first FFT technique, although promising, will also not be initially employed in our studies because of amplification and calibration issues. The second incremental technique will be employed in our studies because modern electronic detectors exhibit the sensitivity to design and build an extremely simple circuit to measure the complex capacitive reactance, as in Fig. I01.

Modern electronic detectors, such as vector voltmeters, lock-in amplifiers, and phase discriminators, contain state-of-the-art solid-state instrumental and operational amplifiers (op.amps.) coupled to digital-signal processing (DSP). Modern op.amps. have much broader frequency response ranges and well

calibrated common-mode rejection ratios (CMRR). The CMRR allows the op.amp. to increase the gain of a input signal without introducing noise into the output, thus allowing op.amps. far greater sensitivity and amplification. Once the raw analog signal is amplified through modern op.amps., the detector can deploy digital circuits and calculations to pull from the preprocessed signal only the signal of interest, therefore, ignoring all noise in and around the true signal. The DSP output can be directly fed to a computer for further acquisition, storage, and analysis.

The Ametek 7265 DSP lock-in amplifier will be used as the voltage source and simultaneous measure the complex current. The 7265 will amplify the signal to better than 100 dB CMRR and then digitally process the amplified signal for a maximum current sensitivity down to 2 fA. Our initial studies prove that our current range will be on the order of 3 to 300 pA, therefore, we are well within the detection range of the 7265 lock-in amplifier.

In other words, a simple capacitive circuit containing a voltage source of stable sinusoidal frequency, from the 7265, is fed into a custom capacitive sample holder. The complex current is then detected through the sample by the 7265 lock-in amplifier yielding the complex impedance of the sample cell. The measurement of the complex current or impedance, in comparison with a second identical vacuum or air capacitive holder, will yield the complex permittivity of the peptide or protein sample. The molecular dipole and solvent effects of the peptide or protein response from the measured complex permittivity is outlined under the Theoretical and Biological Molecules section.

National Instruments provides LabView, an excellent development suite and programming language specifically designed for laboratory and instrument use. LabView will be used to create a custom user interface and control panel within the computer to control all aspects of the physical instrument. LabView will provide an interface to control the frequency range and voltage across the capacitive circuit of a spectrum and acquire the complex current data from the 7265 detector using a GPIB interface. LabView acquires the real and imaginary current data and stores and processes it in real-time. The data is processed through real-time statistical calculations and plots. A screen shot of the user interface is below.

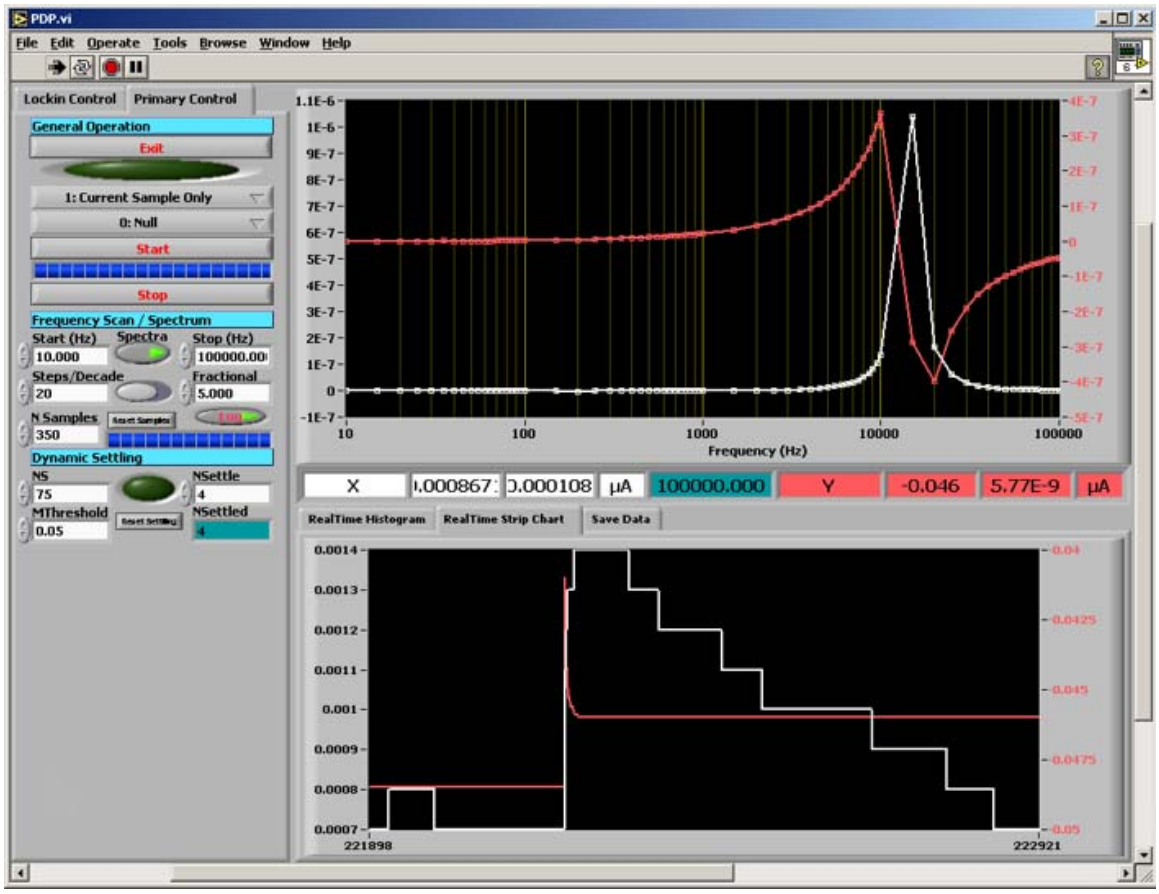

(fig. I02)

where the upper right is a four-decade spectrum of a mica capacitor at room temperature owing to a transition frequency of anomalous dispersion at 14.4 kHz and the bottom right shows a real-time strip chart of the raw data.

The left side of the user interface, split into two tabs, controls all aspects of the physical instrument, as shown in greater detail below.

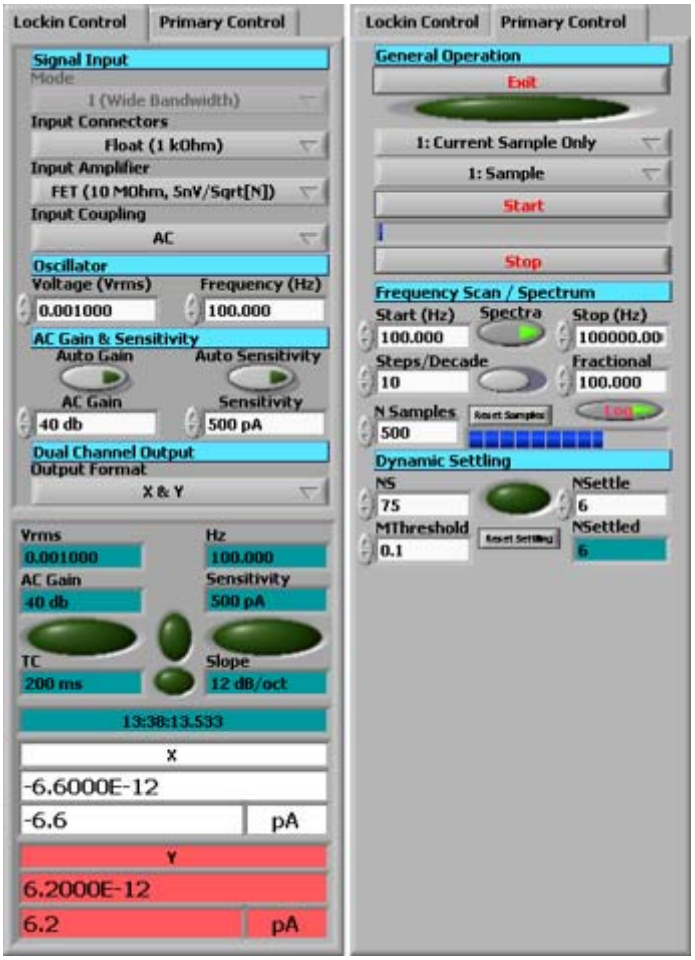

(fig. I03)

The left tab, or "Lockin Control", of the control interface manages the 7265 output voltage, amplification gain, sensitivity range, and frequency, as well as other instrument controls. The bottom of the tab reports any GPIB communication, signal processing, and sensitivity errors from the 7265 with indicator lights. It also reports current settings of the instrument and the complex current data, as well as its magnitude and units.

The right tab, or "Primary Control", of the control interface manages the frequency run, either single frequency or an entire spectrum. It allows for single or multiple decade ranges with a linear or logarithmic mode in which all of the indicators and graphical spectra follow suit. The interface also allows for control over the steps or resolution of a spectrum, the number of samples for averaging per frequency, and dynamic settling. Dynamic settling is for the frequency range less than 10 Hz where the circuit and instrument must settle into a stable complex current reading.

The raw data can be fed into a strip chart, as shown below, to allow for a signal vs. noise comparison in real-time. The numbers above the strip chart report the average and standard deviation for both the real (X in white) and the imaginary (Y in pink) current, as well as the units.

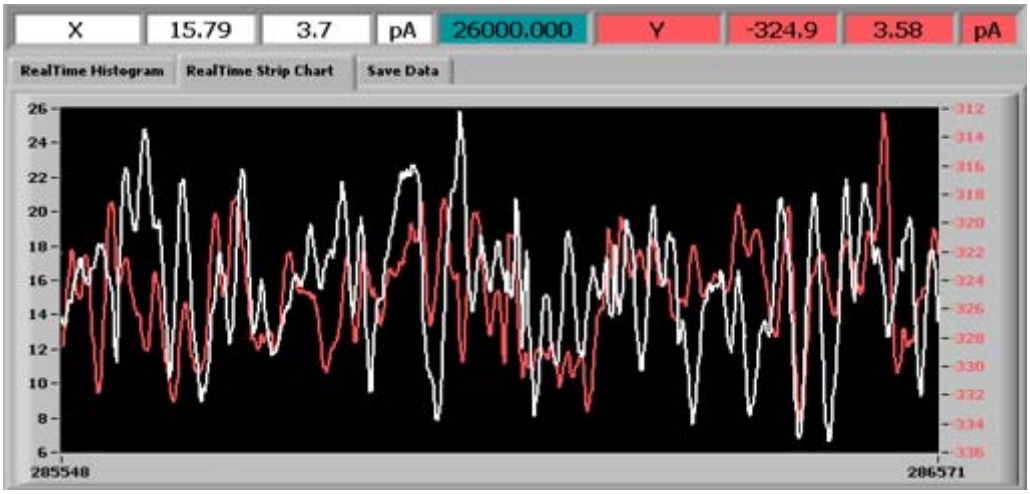

(fig. I04)

LabView also allows the raw data to be fed into a real-time histogram, which is also expressed in complex X, real and white, and Y, imaginary and pink, form, as shown below. These two visualizations are invaluable for gauging the signal to noise ratios and the responses of various samples and circuit designs.

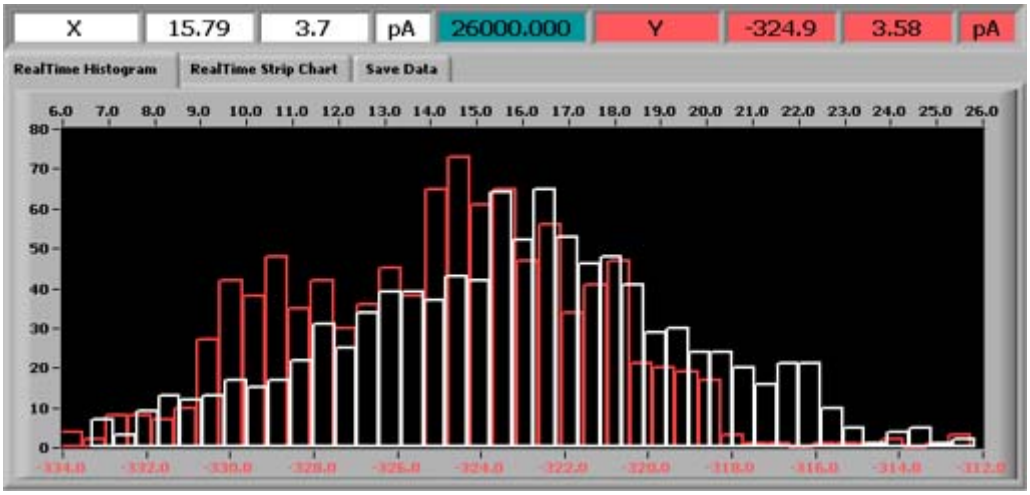

(fig. I05)

And finally, the user interface allows for the full acquisition and storage of all raw and statistically processed data into in-memory arrays. The arrays are used for storage onto computer disk and allow for the real-time graphical display of a spectral run, as shown below

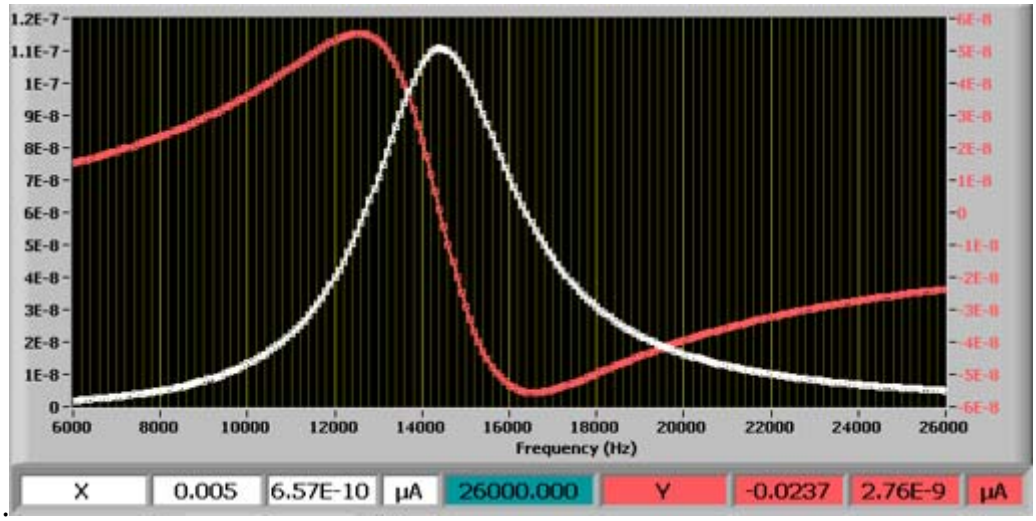

(fig. I06)

The above complex current-based spectrum shows the distinctive anomalous dispersion in pink and the absorption in white.

As a cool aside, the source code for LabView is completely graphical. An example of the PDP's source code is below.

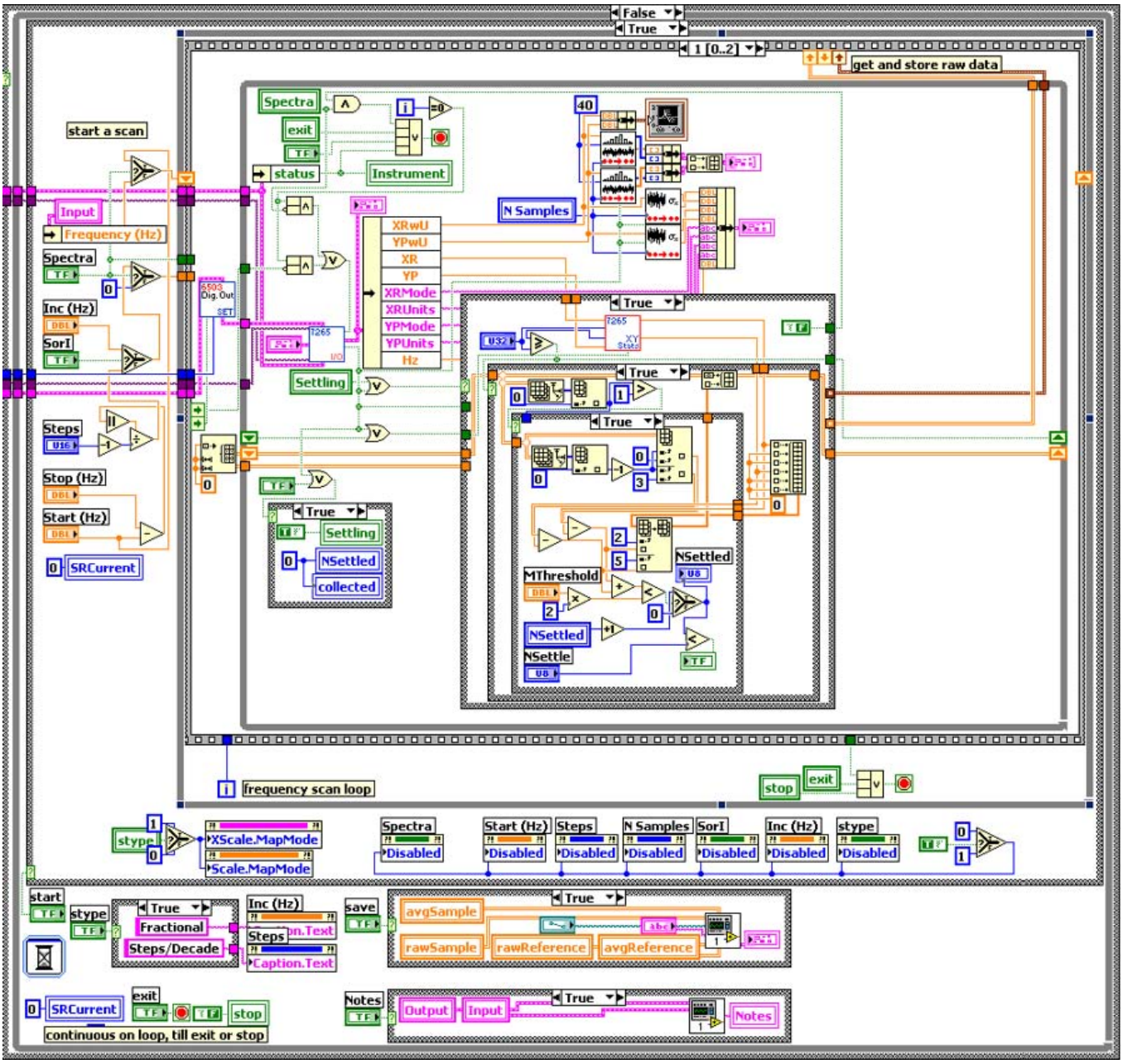

(fig. I07)

The sample holder of the Phase I Dielectric Spectrometer (P1DS) consists of a plexiglass holder with a bored out 1" diameter cylinder, Figure I08. Both open ends of the holder have cylindrically based bronze inserts to act as the capacitive electrodes, in which the minimum separation of the parallel plate electrodes is less than 1/32", and adjustable using cylindrical-disk shims. The sample holder, therefore, will exhibit a volume of approximately 4/10 ml. O-rings are used to ensure a liquid tight seal and an ultrasonic vibrator is used to shake air bubbles from the holder.

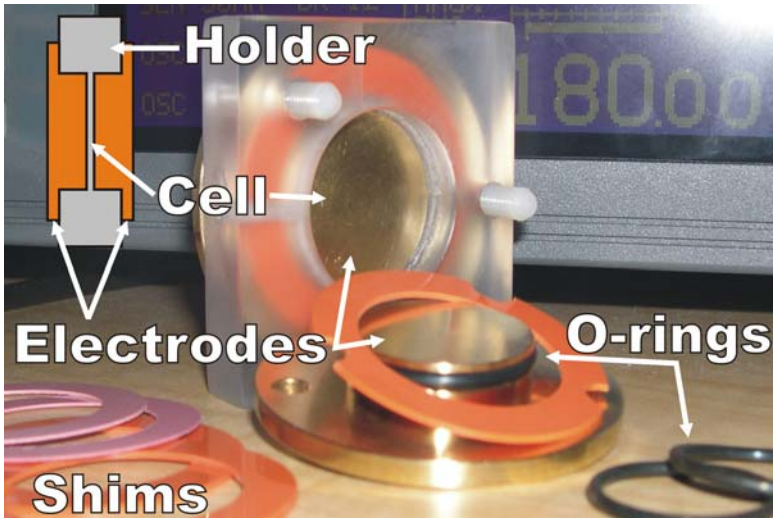

(fig. I08)

The last few months have produced encouraging results from the Phase I Dielectric Spectrometer (P1DS). Also, many new phenomena have been observed. The first natural study is on a vacuum or air sample. The full-range complex admittance is below.

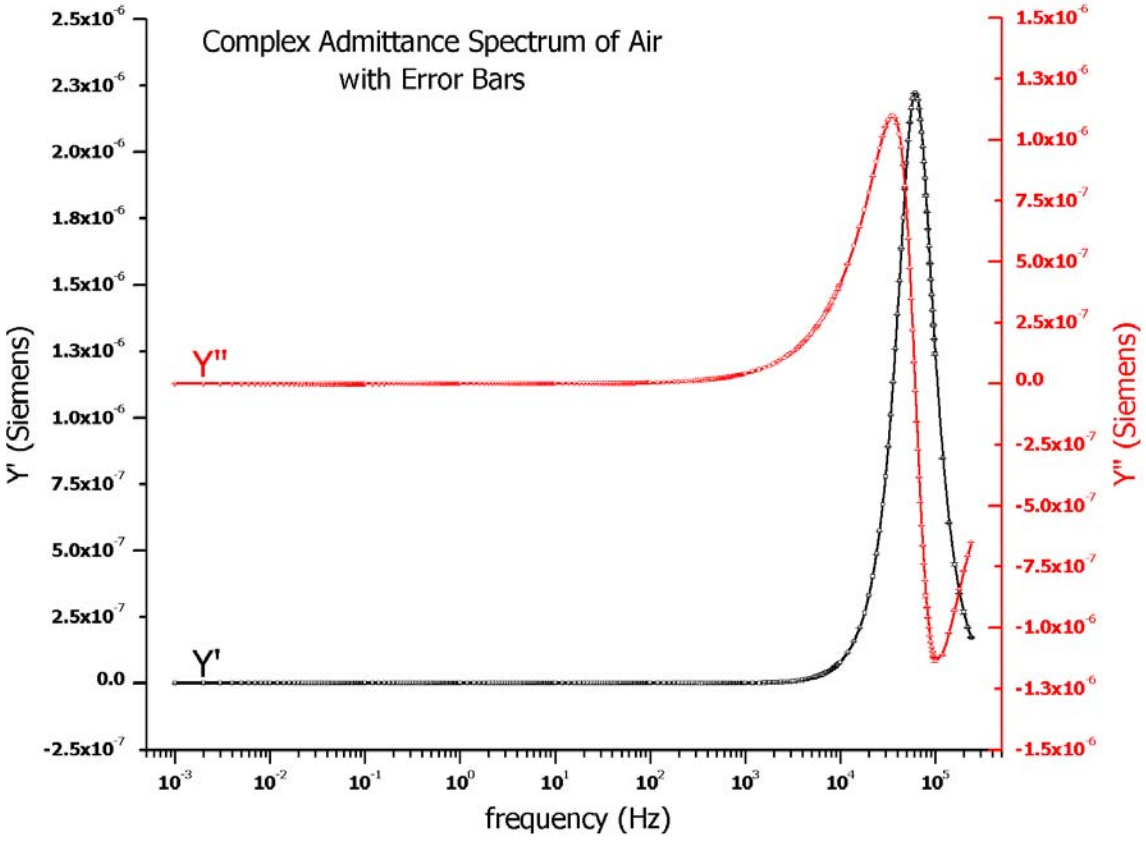

(fig. I09)

As can be seen in Figure I09, both the real and imaginary components of the admittance are well-defined mathematical functions with the expected anomalous dispersion characteristics. The error is also reported in the above plot, revealing the extreme sensitivity and reproducibility of the P1DS. The dispersion detected at 62 kHz, however, should not be observed and is probably due to stray or parasitic effects within sample cell, cabling, or amplifiers. Future spectrometers will require better cabling and specially designed circuits to encompass better guarding and shielding. A lack of effective guarding was the major cause of the above stray effect.

Most dielectric studies of peptides and proteins will be performed in aqueous solution. Therefore, the next natural study is the admittance of pure water, as shown below.

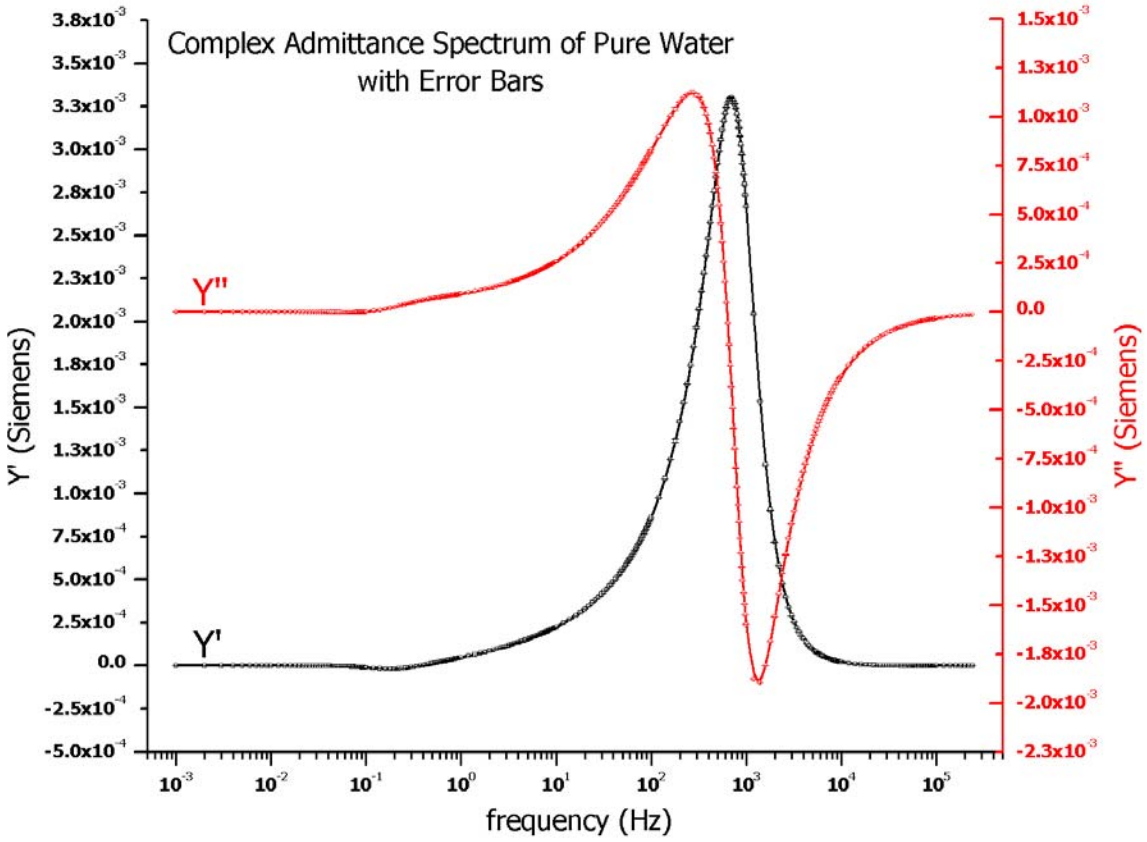

(fig. I10)

As can be seen, the admittance magnitudes of water can be three orders of magnitude greater than that of air. The expected result should be a constant eighty times greater within this frequency range. The dielectric constant of water is a constant eighty until around 1 GHz. The peaks reported in Figure I10 are probably due to electrode polarization effects, for the dispersion occurs in the frequency range reported by previous studies. Electrode polarization will need to be decreased or negated in future spectrometers and techniques.

Hemoglobin was then studied in aqueous solution. The complex admittance is below in Figure I11.

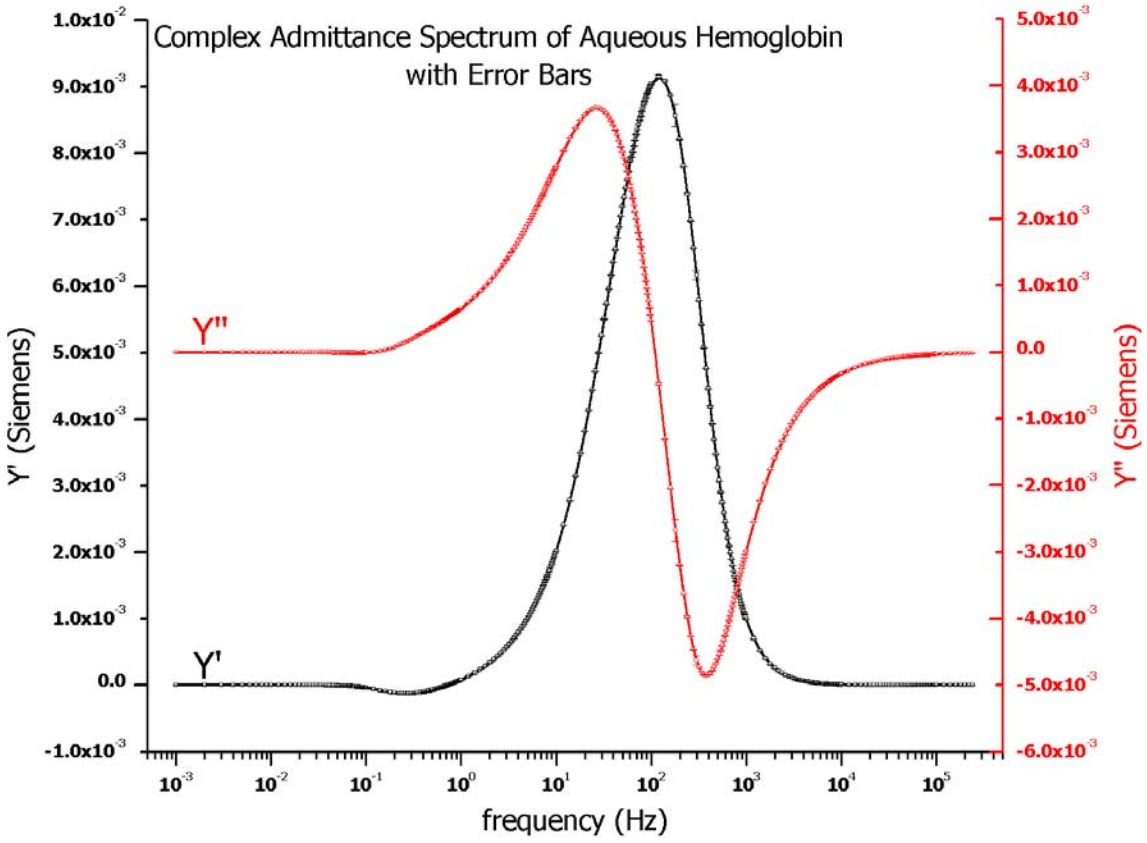

(fig. I11)

As can be seen the stray admittance of the air sample is far lower than discernable in either the pure water to the aqueous hemoglobin. The aqueous hemoglobin has a similar dispersion due to electrode polarization than that of pure water. However, the dispersion is shifted to a lower frequency and the peak is broadened. This is to be expected for electrode polarization effects for aqueous hemoglobin.

Dividing the complex admittance of the aqueous hemoglobin over that of pure water, or using Equations I14 at each frequency point, the following complex dielectric spectrum is derived for aqueous hemoglobin.

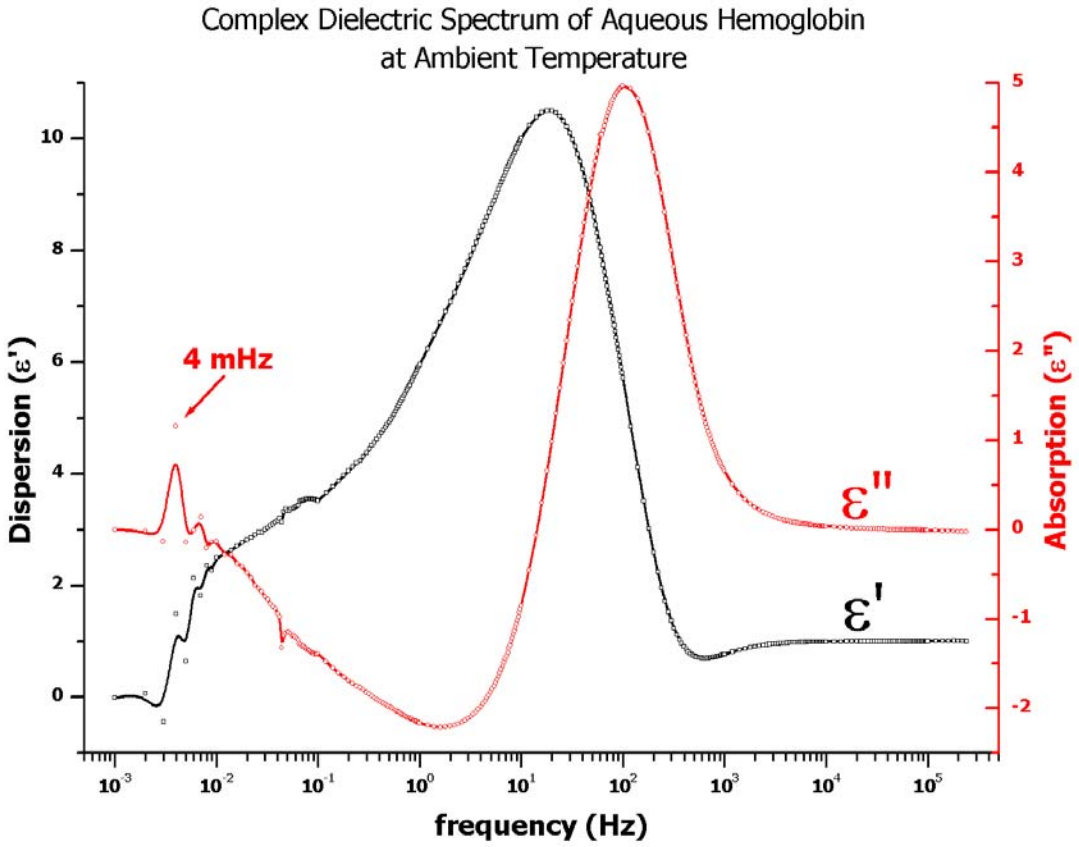

(fig. I12)

where the large dispersion due to electrode polarization is centered at 100 Hz and is still prevalent compared to the admittance spectrum. An interesting phenomena, however, appears at less than 20 mHz. A rather obvious absorption peak occurs which is shown in the imaginary permittivity and centered at 4 mHz. It is characterized by normal dispersion as revealed by its real permittivity. Normal dispersion has only been generally observed in the infrared, optical, or ultra-violet regions of the electromagnetic spectrum. Traditionally, normal dispersion is attributed to resonant processes, whereas anomalous dispersion is attributed to relaxation processes.

The data is clear in revealing that the 4 mHz absorption peak is a primary peak and harmonics can be distinguished at approximately 8, 12, and 16 mHz. This is additionally confirmed in the real dielectric spectrum. Therefore, the data apparently reveals normal dispersion and harmonics in the region from 4 to 16 mHz, with the primary peak at 4 mHz. Initial interpretation can attribute the observed data to resonance effects due to intramolecular dielectric responses of structural motifs or to dielectric responses of hydration layers within or directly surrounding the protein.

The ultra-low frequency dielectric spectrum of pure dry flakes of hemoglobin was performed to confirm the above results. The data is shown in Figure I13.

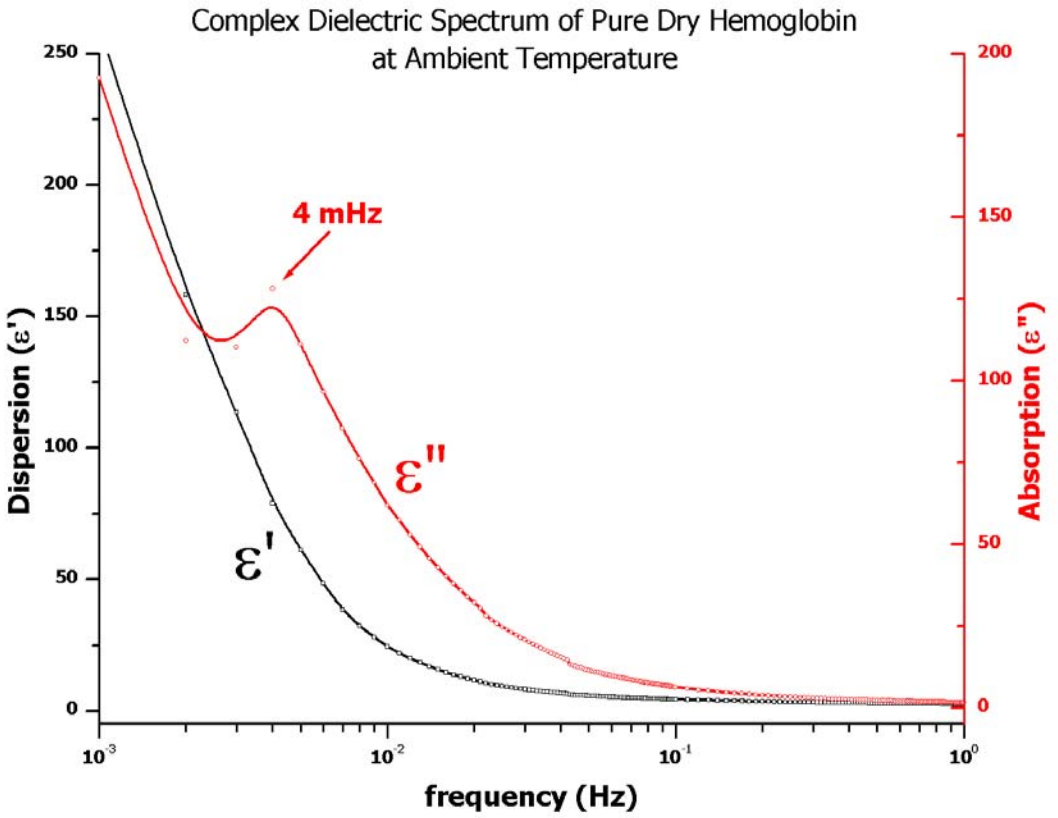

(fig. I13)

The absorption peak at 4 mHz is apparent, albeit the harmonics are not distinguishable. The dry studies of hemoglobin would negate any electrode polarization effects, for these are due to mobile charge or ion carriers, such as that found in solution. Also, the great majority of the immediately external and surrounding hydration layers would not exist, thus the 4 mHz response must be attributed to either a dielectric response of the intramolecular structural motifs or to the response of protein-embedded water. Therefore, it can concluded that the 4 mHz dielectric response is due to a intramolecular dielectric response of hemoglobin. Since the frequency resolution of the P1DS is only 1 mHz, the exact location of the primary and harmonic peaks can not be accurately determined. Further study is required in this frequency region.

Proposed Dielectric Spectrometers

Phase II & III Dielectric Spectrometers

The proposed Phase II and III Dielectric Spectrometers (P2DS and P3DS) will be designed to increase the overall stability and reproducibility of the dielectric spectrum within the range of 1 mHz to 102 kHz. It was found with the water and gelatin studies of the above P1DS that the detected signal must be further stabilized to ensure reproducible accurate results, thus a few things require further attention.

First, a different off-the-shelf lock-in amplifier should be used which is traditionally more reliable. Conversations with Paul Moses at the Center for Dielectric Studies at PSU brought forward that the Stanford Research SR830 DSP Lock-In Amplifier should be used to replace the Signal Recovery 7265 DSP Lock-In Amplifier, thus phasing out the P1DS altogether.

Although David Ames at Stanford Research suggests that the standard current-to-voltage (I-to-V) converter in the SR830 should be sufficient, the second upgrade, with the employment of the SR830, is to create a specialized converting preamplifier. The preamplifier is critical for impedance matching of the sample cell to the lock-in amplifier. In fact, the preamplifier may need to be "smart", in the sense that at lower frequencies, probably less than 1 or 10 Hz, the preamplifier will need to be more of a charge-to-voltage converter. This is essentially a capacitive integrating operational amplifier. And then, at higher frequencies, above 1 or 10 Hz, the converter would be a more standard resistive gain operational amplifier. The "smart" preamplifier may need to switch between the two configurations depending on the frequency of the current measurement.

The third upgrade will include electrical shunts to ground of the generator and detector signals when the spectrometer is changing frequencies. It has been realized that excluding such a shunt, as in the P1DS, causes the previous frequency to additionally superimpose on the frequency currently under study. At frequencies above 100 Hz this is not an issue because the previous signal will decay very fast. However, at lower frequencies the persistence of the previous signal is appreciable and observable, with the decay rate decreasing exponentially as the frequency decreases. It has been observed in the P1DS that the previous frequencies can greatly affect, because of the decay rates and superimposition, the accurate dielectric measurement at the current frequency. Therefore, low frequencies studies require a "cleaning", by using the shunt to ground, of the excitation and detector cables to ensure that the previous signals are completely removed from the experiment.

The fourth upgrade would be to fabricate new sample cells that include guarding, with better shielding and grounding. The inclusion of guarding will ensure that outer fringe effects of the electric field through the sample cell will be excluded from the measured signal. The guarding will ensure that the measured permittivity is consistent between different samples. Overall, redesigning the sample cells with these three criteria will greatly reduce or fully negate stray, parasitic, or transient electronic effects, those usually produced from electronic components, therefore increasing the sensitivity and reproducibility on the side of the sample cells.

Currently, the P1DS requires a scan of the reference cell, and then a separate scan of the sample cell. The time between the two scans can be twelve or more hours, which can introduce huge errors in the

dielectric calculation, Equation I14, due to environmental changes between the two scans. Therefore, the fourth upgrade would require the use of two SR830 amplifiers, in parallel, to allow the simultaneous excitation and measurement of the impedance of each sample cell. This would allow, for example, one sample cell to be the reference, while the other is the sample. The impedance of both would lead to the complex dielectric, as shown in Equations I11 through I14. The simultaneous study of parallel sample cells would exclude any deviations due to the environment, i.e. temperature or humidity.

It was also realized that the mechanism of coating Pt-Black on the electrodes to reduce electrode polarization is the generation of a thin layer of hydrogen gas between the sample cell electrode and the sample itself. Since hydrogen is a nonpolar substance, it would act as a conductive barrier between the sample and the electrode, therefore greatly reducing the effects of electrode-polarization. It is proposed to study the effects of various petroleum-based substances on the electrodes to reduce the effects of electrode polarization. These studies would be critical since most of the peptide and protein samples will be in aqueous solution. Therefore, reducing the overwhelming effect of conductive water on the electrodes is essential for studies of peptide and proteins in aqueous solution.

The SR830 will be the primary signal generator and detector for the P2DS. The LabView software from the P1DS will require some upgrading, however, this will be fairly simple and straightforward. It is estimated that the software upgrade will require less than a few weeks of programming.

Similarly, the Stanford Research SR785 Dynamic Signal Analyzer will be employed for the P3DS. It has a frequency range of DC to 102 kHz. The SR785 uses pulsed or fourier-transform technology to measure the dielectric response of the sample cells. The employment of the SR785 in the P3DS would allow for high-energy excitation studies on peptides and proteins. This may be critical since the non-linear and harmonic responses may be more important than the primary response of the peptide and protein samples. Additionally, the SR785 has two independent signal inputs, therefore, two samples cells can be excited and measured in parallel and simultaneously, thus only a single SR785 is required.

The proposed spectrometers will push the limits of off-the-shelf technology to detect and characterize the intramolecular dielectric responses of peptides and proteins. This understanding will propel our biophysical and biochemical understanding of peptides and proteins, and living systems, in general.

Phase IV Dielectric Spectrometer

The Phase IV Dielectric Spectrometer (P4DS) detector will be based on a Tektronix TDS5104 1-GHz 4-Channel Digital Oscilloscope with an expected frequency range of 1 μHz to 240 MHz. The idea is to use a commercial oscilloscope as the detector. Custom amplifiers will be used to boost the gain of the input signals. The first signal will be a direct connection to the generator, in which it will act as the primary reference signal, by comparison, for the measurements. Three additional signal inputs can then be coupled to three separate and independent sample cells, thereby allowing for simultaneous and parallel, and thus accurate, dielectric measurements.

The P4DS will require one or two function generators, the sample cells, custom amplifiers, the oscilloscope, a PC, and National Instruments LabView. The generators will be used to excite the sample cells, in which the amplified analog signal is converted to a digital signal by the oscilloscope. The PC

will be connected to the oscilloscope through a GPIB interface and LabView will acquire the digital waveforms from the oscilloscope.

The primary challenge of the P4DS will be to convert an oscilloscope into a lock-in amplifier, impedance analyzer, or complex-channel dielectric spectrometer. It is proposed to extensively use LabView to perform all digital computations and real-time analysis, statistics, and graphics. Since LabView comes with extensive real-time computational and statistical packages, it can be used to massage and display the digital waveforms as a lock-in amplifier, impedance analyzer, and/or dielectric spectrometer. The final LabView program will have an extensive user-interface to allow the user to choose the mode and measurement type for the particular experiment.

For instance, if a single frequency is applied to the sample cells, the P4DS can be used as a lock-in amplifier. Magnitude and phase differences can be calculated by comparison to the primary reference signal to provide the conductivity, the real component, and capacitance, the imaginary component, of the sample cells. Dielectric spectra can be obtained in this mode by incrementally scanning a frequency range. This method of dielectric measurement and spectrum acquisition is analogous to that used in the P1DS and P2DS.

Another example, would be to apply a single frequency to the sample cells, as in the latter paragraph, however, use the P4DS in a spectrum mode. The digital waveform of the sample can be massaged through a fast Fourier-Transform (FFT) calculation to convert the natural time-domain of the digital waveform to the frequency-domain, thereby being a real-time spectrum. Since the applied frequency is a narrow single frequency, the FFT would quickly reveal any harmonic or nonlinear responses. This method would also excel with high excitation voltages because the oscilloscope has a much higher saturation level than the lock-in amplifiers of the P1DS and P2DS. These types of measurements have never been performed on peptides and proteins.

And a finally, the P4DS can apply a predefined pulse, square, gaussian, etc., to the sample cells and perform a FFT calculation to reveal the dielectric spectra. Applying a pulse is like hitting the sample with a broad range of frequencies simultaneously. Measuring and observing the peptide and protein responses using this method could reveal other phenomena never before seen. This method is the same method as FT-IR spectroscopy, or Fourier-Transform Infra-Red Spectroscopy. In fact, it is the pulsed and FFT techniques used in modern IR spectroscopy that make this method so fast and reliable.

Although the P4DS will not have the sensitivity as the P2DS and P3DS, it will provide a far greater frequency range, multiple modes and methods of measurement depending on the experiment and desired results, higher excitation voltages without saturation, observe nonlinear and harmonic responses with ease, and observe multiple frequencies and responses simultaneously generated by different aspects of the same sample cell.

Phase V Dielectric Spectrometer

The Phase V Dielectric Spectrometer (P5DS) will be a new creation based on lock-in amplifier technology. The idea is the create a lock-in amplifier, from the ground up, that out performs all commercially-available lock-in amplifiers. The lock-in amplifier will form the natural foundation so

that the final instrument will also be a practical impedance/admittance analyzer and dielectric spectrometer.

The first step to creating the P5DS will be to completely model and simulate the circuits of a new DSP lock-in amplifier using the latest circuit analysis software, Cadence OrCad Unison. The overall technical objectives of the P5DS are:

1. encapsulate the frequency range from 1 μHz to 250 MHz,
2. increase the sensitivity, stability, and reproducibility as compared to off-the-shelf lock-in amplifiers,
3. design an arbitrary oscillator that generates superimposed multiple excitation frequencies with concurrent amplification, detection, and reporting each discrete frequency response of the signal,
4. include a Rubidium time base for increased precision and long-term stability,
5. decrease the settling time of low frequency studies by locking in more rapidly,
6. include software and components for self-calibration, self-diagnostics, and operational integrity,
7. modularize the major components for user and application scalability,
8. encapsulate the system into a self-contained user-friendly instrument,
9. include real-time statistical and graphical tools for end-user monitoring, analysis, and advanced control of the instrument,
10. and, automate incremental frequency scanning for complex admittance, impedance, or dielectric spectroscopies.

The P5DS will have an algorithmic form of:

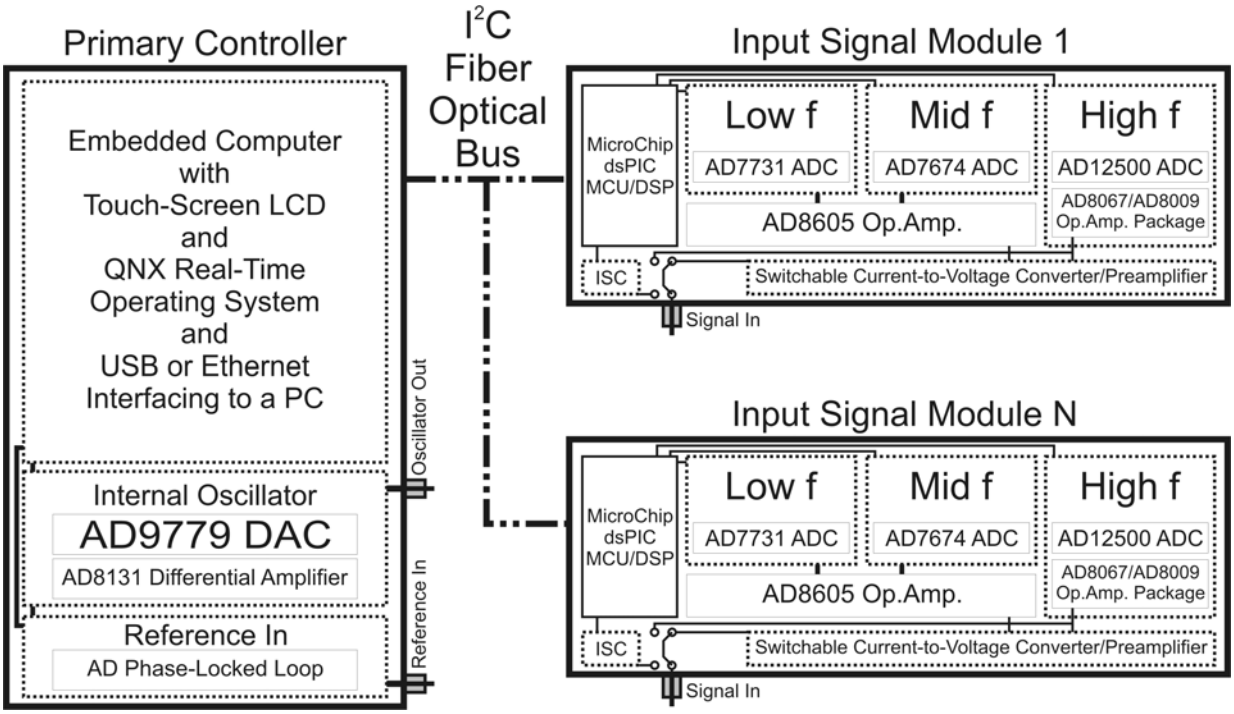

Once the P5DS is completely designed and simulated in the computer, and meets the technical specifications and expectations, then the circuit boards will be fabricated and the software installed and programmed. Much of the software processes and algorithms used to create the P4DS will be used in the software for the P5DS.

Essentially, the P5DS will possess all of the best aspects of the P1DS through P4DS of greater sensitivity, stability, precision, reproducibility, frequency range, automation, and multiple simultaneous sample cells within a single instrument, and provide a few new aspects of multiple simultaneous excitation frequencies and time-base stability.

Annual Objectives and Proposed Budgets

The first generation Phase I Dielectric Spectrometer (P1DS), with a frequency range of 1 mHz to 250 kHz, has been built and successfully operating since mid 2004. It has proven that dielectric measurements can be achieved at room temperature with gelatin, myoglobin, and hemoglobin. This work could not have been achieved without the corporate support of Ametek, National Instruments, Tektronix, 3M, Mettler-Toledo, and Millipore Corporation. Their gracious contributions, totaling over $50,000, have propelled the PDP to new and unexpected heights.

2006 Annual Objective and Budget

The primary objective for 2006 is to further develop the electronics, software, and sample cells to confirm our previous findings, as well as, progress the chemical techniques and sample preparation to amplify the dielectric signatures of the structural motifs of peptides and proteins. It is intended to use off-the-shelf voltage sources, amplifiers, and detectors, coupled with in-house programming for real-time computational and instrumental control, to create the next generation of dielectric spectrometers, the Phase II through IV Dielectric Spectrometers (P2DS – P4DS). The culmination of these three spectrometers will increase the frequency range from 1 μHz to 240 MHz with a marked increase in stability and reproducibility of the measured signal.

The P2DS will consist of two coupled Stanford Research SR830 DSP Lock-In Amplifiers, new dielectric sample cells, a PC, and LabView. These amplifiers have a frequency range of 1 mHz to 102 kHz and possess the greatest noise-filtering capabilities, and thus sensitivity, and measurement stability of any amplifier on the market. Two amplifiers are required to allow for simultaneous measurements of two sample cells. The simultaneous measurements will greatly increase the accuracy of the final dielectric spectra.

The P3DS will consist of a Stanford Research SR785 Dynamic Signal Analyzer, new dielectric sample cells, a PC, and LabView. This analyzer can detect a dielectric signal in the frequency range of DC to 102 kHz. Although this signal analyzer does not possess the sensitivity as the amplifiers of the P2DS, it can reach down into the μHz range and perform measurements at a far greater rate than the P2DS. Also, a single analyzer allows for simultaneous measurements for accurate dielectric spectra, as similarly proposed for the P2DS.

The P4DS will consist of two signal sources, the Agilent 33250A and the Tektronix AFG3252 Arbitrary Function Generators, a Tektronix TDS5104 1-GHz 4-Channel Digital Oscilloscope, a Fluke PM6681R High Performance Frequency Counter, new dielectric sample cells, a PC, and LabView. Two signal sources are required to effectively span the frequency range of 1 μHz to 240 MHz. Although the P4DS has less noise-filtering capability, and thus less sensitivity, than the P2DS or the P3DS, it has a far greater

frequency range and will allow for high voltage or excitation studies of peptides and proteins. This spectrometer will require the greatest software development because it is through the use of the PC and LabView that the TDS5104 Oscilloscope and the PM6681R Frequency Counter will be coupled together to act as a single high-performance detector, therefore creating a new type of dielectric spectrometer. Additionally, the 4 channels of the oscilloscope will allow for up to four simultaneous measurements, thereby accurately determining the dielectric spectra in four sample cells, as similar in the P2DS and the P3DS.

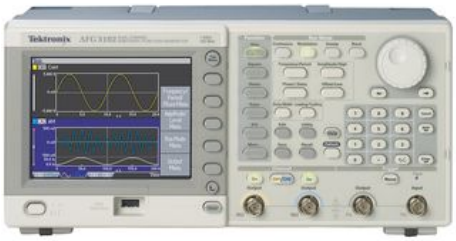

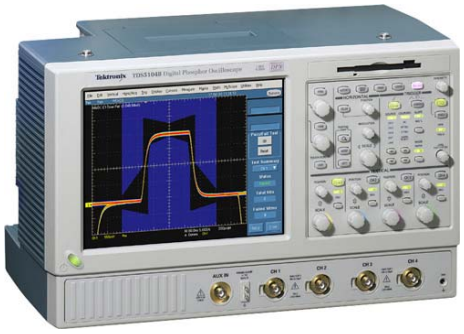

The beforementioned LabView, manufactured by National Instruments, is the premier development software for research quality instrument control, data acquisition, and real-time data and graphical analysis. This software is essential for developing the computational and analytical routines necessary for the Phase I to Phase IV Dielectric Spectrometers.

New dielectric sample cells will be designed and fabricated to interface with the four abovementioned dielectric spectrometers. The samples cells will be designed with proper guarding, shielding, and grounding to maximize the dielectric signal from the peptide and protein samples. They will be initially used for room temperature studies, but designed and built to interface with a solvent-based temperature controller slated for the next year.

And finally, the Fluke PM6306/563 RCL Meter will provide fast accurate confirmation of the empty sample cells for null readings, as well as, provide a quick reference check on new samples and sample preparations.

Qty.	Make	Model	Description	Unit	Rqr'd	Extended
2	SRS	SR830	DSP Lockin Amplifiers	$3,950.00	Y	$7,900.00
1	SRS	SR785	Dynamic Signal Analyzer	$14,350.00	Y	$14,350.00
1	Agilent	33250A	Low-Frequency Signal Generator	$4,553.00	Y	$4,553.00
1	Tektronix	AFG3252	High-Frequency Signal Generator	$8,500.00	Y	$8,500.00
1	Tektronix	TDS5104	1-GHz 4-Channel Digital Oscilloscope	$18,500.00	N	$0.00
1	Fluke	PM6681R/476	High-Precision Frequency Counter	$16,245.00	Y	$16,245.00
1	Fluke	PM6306/563	RCL Meter	$6,580.00	Y	$6,580.00
1	Millipore	Elix5&MilliQ	Ultra-High-Purity RO Water Filtration	$18,000.00	N	$0.00
1	Mettler-Toledo	S47	pH/Conductivity Meter with Probes	$3,213.05	Y	$3,213.05
1	Mettler-Toledo	AT261	Analytical Balance	$8,500.00	N	$0.00
1	Nemetschek	VectorWorks	VectorWorks 12 CAD Mechanical	$1,885.00	N	$0.00
1	NI	LabView	LabView Full v7.1 with GPIB Interfacing	$4,800.00	N	$0.00
1			Sample Cell Materials and Fabrication	$2,500.00	Y	$2,500.00
1			Peptides, Proteins, Gels, Agaroses, Etc.	$1,000.00	Y	$1,000.00
						$64,841.05

In summary, the primary objective for 2006 centers on integrating the off-the-shelf electronics and software for three new dielectric spectrometers, the P2DS to P4DS, with the secondary objective centering on the sample cell design and calibration.

2007 Annual Objective and Budget

The objectives for 2007 are quite different then 2006. This year, the primary objective centers on the chemical techniques for peptide and protein sample preparation and sample cell design and physical control. The secondary objective for 2007 will be to begin development of a completely new DSP lock-in amplifier, which will form the basis of the Phase V Dielectric Spectrometer (P5DS). The P5DS development will be engineered from the ground up, using the latest circuit analysis techniques in specially designed software.

The primary objective of developing the chemical and physical techniques for sample preparation and sample cell control will be carried out by myself, Lucas. Temperature control and precision will be applied to the sample cells by employing a nonpolar solvent-based refrigerated/heated external circulator to the sample cells. The Julabo FP50-ME will control the temperature of the sample cells from –50 to 200°C with 0.01°C stability. Studies can be performed on super-cooled aqueous samples (<0°C) and the structure motifs as the proteins begins to unfold at the warmer denaturization temperatures (~40-70°C) for those proteins. These temperature-based studies will be crucial to understanding the structural and catalytic effects of the applied electric field on the internal dynamics of the protein. They will also aid in determining the fictional factors of neighboring structural motifs at various temperatures within the protein. These are studies that have never been previously explored or reported.

The secondary objective of designing and analyzing the new circuits for the P5DS will be performed by Travis Carter. Briefly, Travis is an EMI expert with extensive education and experience in electronic design and implementation. Travis will completely model and simulate the circuits of a new DSP lock-in amplifier using the latest circuit analysis software, Cadence OrCad Unison. The objectives of the P5DS are:

1. encapsulate the frequency range from 1 μHz to 250 MHz,
2. increase the sensitivity, stability, and reproducibility as compared to off-the-shelf lock-in amplifiers,
3. design an arbitrary oscillator that generates superimposed multiple excitation frequencies with concurrent amplification, detection, and reporting each discrete frequency response of the signal,
4. include a Rubidium time base for increased accuracy and long-term stability,
5. decrease the settling time of low frequency studies by locking in more rapidly,
6. include software and components for self-calibration, self-diagnostics, and operational integrity,
7. modularize the major components for user and application scalability,
8. encapsulate the system into a self-contained user-friendly instrument,

9. include real-time statistical and graphical tools for end-user monitoring, analysis, and advanced control of the instrument,
10. and, automate incremental frequency scanning for complex admittance, impedance, or dielectric spectroscopies.

The P5DS will have an algorithmic form of:

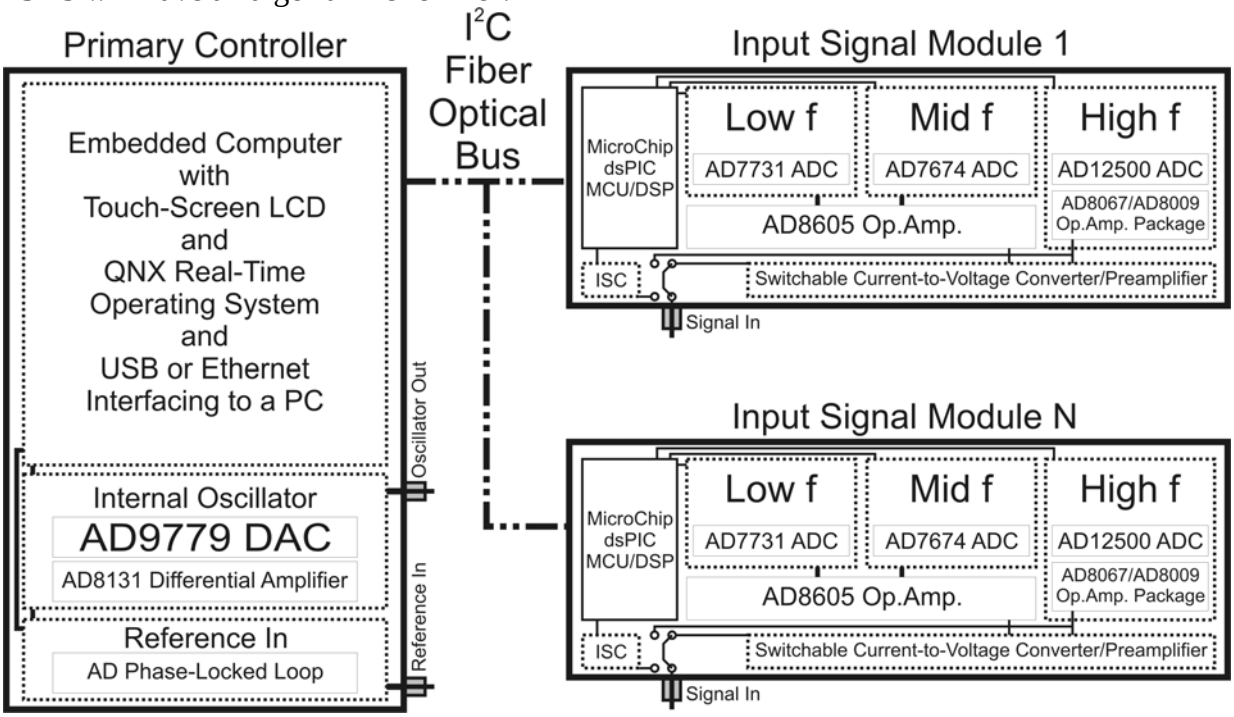

Essentially, the P5DS will possess all of the best aspects of the P1DS through P4DS of greater sensitivity, stability, reproducibility, frequency range, automation, and multiple simultaneous sample cells within a single instrument, and provide a few new aspects of multiple simultaneous excitation frequencies and time-base stability.

Qty.	Make	Model	Description	Unit	Rqr'd	Extended
1	Julabo	FP50-ME	Refrigerated/Heating Circulator [-50,200]C	$7,560.00	Y	$7,560.00
1	Orion	555A0	pH/Conductivity Meter with Probes	$2,896.00	Y	$2,896.00
6	Eppendorf	2100	Volumetric Pipettes, Single Channel Adjustable	$289.00	Y	$1,734.00
1	Eppendorf	2100	Carousel Stand for Volumetric Pipettes	$111.00	Y	$111.00
1	Cadence	OrCad Unison-Ultra	PSpice Analog & Digital Circuit Design & Simulation Software	$9,995.00	Y	$9,995.00
1	Consulting	Travis Carter	Lock-In Amplifier Development and Simulations in OrCad	$10,000.00	Y	$10,000.00
1	OriginLab	OriginPro	OriginPro 7.5 with Peak-Fitting Plug-in	$588.00	Y	$588.00
1			Sample Cell Materials and Fabrication	$2,500.00	Y	$2,500.00
1			Peptides, Proteins, Gels, Agaroses, Etc.	$4,000.00	Y	$4,000.00
						$39,384.00

In summary, the primary objective for 2007 centers on the chemical techniques for peptide and protein sample preparation and sample cell design and physical control using the electronics of the P2DS

through P4DS. The secondary objective is to design and simulate the circuits of a brand-new lock-in amplifier, which will naturally lead to the creation of the P5DS.

2008 Annual Objective and Budget

The third year of research will be a direct continuation of the second year of research. The priority of the objectives will most likely switch, wherein the primary objective will focus on the P5DS and the secondary objective will further the sample cell development and preparation.

The previous year, 2007, will be devoted to designing and simulating the P5DS circuits in high-end circuit analysis software. This will include simulating noisy input signals to determine the noise-filtering, stability, and reproducibility of the proposed new circuits. Once the simulations are successful in 2007, then in 2008, the circuits will be fabricated, tested, and calibrated to ensure that the lock-in amplifier meets specified expectations. Therefore, in 2008 it is proposed to build the new DSP lock-in amplifier, which will then lead to the P5DS.

In short, the P5DS will comprise a central processing station that is composed of an embedded computer running the QNX operating system. LCD Touch-Screens will be the primary user-interface. The central station will also generate the excitation frequencies from its own high-precision internal oscillator or function generator. An external source can also be used and fed into the reference input. Multiple input signal modules may communicate to the central station through a low-noise I^2C fiber-optic communications bus. The multiple input signals will essentially be independent signal processors that relay the pure DSP lock-in data back to the central station for further real-time processing, graphing, statistical analyzing, and reporting on the LCD touch-screen. The multiple input signals will also allow for simultaneous multiple sample cells for accuracy in determining the dielectric spectra.

The secondary objective will be to continue with sample cell design and fabrication, physical control of the samples, and further develop the chemical techniques for sample preparation. It is believed that such chemical and physical techniques are paramount to observing the intramolecular structural motifs within peptides and proteins. It is for this reason that over four years is devoted to this objective.

Qty.	Make	Model	Description	Unit	Rqr'd	Extended
1	Eppendorf	5810	Multipurpose Benchtop Centrifuge	$9,929.00	Y	$9,929.00
1	Lab-Line	3771	General Purpose Refrigerator/Freezer	$1,442.00	Y	$1,442.00
2			Embedded Computer System	$950.00	Y	$1,900.00
2	3M	M170	17" LCD Touch-Screens	$850.00	N	$0.00
1	Pace	PRC2000/E	Precision Surface-Mounting Fabrication Bench	$4,475.00	Y	$4,475.00
1	QNX	Momentics	RT-OS, Modules, and Development Languages	$10,895.00	Y	$10,895.00
1	Olympus	SZX-ZB12	Stereoscope for Circuit Analysis and Sample Cell & Electrode Characterization	$12,474.00	Y	$12,474.00
1			Custom Circuit Materials & Fabrication	$25,000.00	Y	$25,000.00
1			Sample Cell Materials and Fabrication	$5,000.00	Y	$5,000.00
1			Peptides, Proteins, Gels, Agaroses, Etc.	$5,000.00	Y	$5,000.00
						$76,115.00

In summary, the primary objective for the third year of research is to build the P5DS. The secondary objective is to continue with the sample cell development, physical control, and chemical preparation to maximize the signal from the structural motifs within peptides and proteins.

2009 Annual Objective and Budget

The fourth year of development is to continue with the research and development of the prior three years. A highly dynamic solvent-based refrigerated/heated circulator will be coupled to the P5DS, from the previous year. The Julabo LH-85 solvent-based refrigerated/heated external circulator will greatly increase the temperature range as compared to the FP50-ME.

A final Phase VI Dielectric Spectrometer (P6DS), with a frequency range of 25 kHz to 200 MHz, is additionally proposed to confirm the results of the P5DS. The P6DS will employ the Stanford Research SR844 High-Frequency DSP Lock-In Amplifier, the Tektronix AFG3252 Arbitrary Function Generator, a PC, and LabView. The development of the P6DS will be similar as that used to build the P1DS and the P2DS. Although the P6DS will not have the sensitivity or stability as the proposed new P5DS, it should still be employed to ensure proper confirmation of sample cells and peptide and protein responses.

Qty.	Make	Model	Description	Unit	Rqr'd	Extended
1	Jubalo	LH-85	Refrigerated/Heating Circulator [-85,400]C	$23,375.00	Y	$23,375.00
2	SRS	SR844	25 kHz to 200 MHz Lock-In Amplifier	$7,950.00	Y	$15,900.00
1	Tektronix	AFG3252	High-Frequency Signal Generator	$8,500.00	Y	$8,500.00
1			Sample Cell Materials and Fabrication	$5,000.00	Y	$5,000.00
1			Peptides, Proteins, Gels, Agaroses, Etc.	$2,500.00	Y	$2,500.00
						$55,275.00

In summary, the primary objective of the fourth year is to continue the research and development, and to confirm the results and analyze the data. It is hoped that by the fourth year, data is clear, distinct, reproducible, irreconcilable, and publishable in scientific journals.

Summary

Impedance or dielectric spectroscopy is the ultra-low energy technique to study charge distributions, polarization, and electrical dynamics in matter. The PDP will develop ultra-sensitive and ultra-low frequency dielectric spectrometers to detect and study the secondary structure and intramolecular structural motifs of peptides and proteins. This will also include the study of intra- and interchain interactions and dynamics within a protein. Once the instrumentation is developed, the study will generate a reproducible array or catalog of dielectric responses of intramolecular structural motifs, thus providing scientists a tool to study proteins in their natural aqueous environment and promoting the fundamental fields of biophysics, biochemistry, and proteomics.

References